Filterbank Transceivers Optimizing Information Rate in Block Transmissions over Dispersive Channels

Anna Scaglione, *Student Member, IEEE,* Sergio Barbarossa, *Member, IEEE,* and Georgios B. Giannakis, *Fellow, IEEE*

***Abstract*—Optimal finite impulse response (FIR) transmit and receive filterbanks are derived for block-based data transmissions over frequency-selective additive Gaussian noise (AGN) channels by maximizing mutual information subject to a fixed transmit-power constraint. Both FIR and pole-zero channels are considered. The inherent flexibility of the proposed transceivers is exploited to derive, as special cases, zero-forcing (ZF) and minimum mean-square error receive filterbanks. The transmit filterbank converts transmission over a frequency-selective fading channel, affected by additive colored noise, into a set of independent flat fading subchannels with uncorrelated noise samples. Two loading algorithms are also developed to distribute transmit power and number of bits across the usable subchannels, while adhering to an upper bound on the bit error rate (BER). Reduction of the signal-to-noise ratio (SNR) margin required to satisfy the prescribed BER is achieved by coding each subchannel's bit stream. The potential of the proposed transceivers is illustrated and compared to discrete multitone (DMT) with simulated examples.**

***Index Terms*—ADSL/HDSL, bit loading, block transmissions, dispersive channels, DMT, filterbank transceiver design, OFDM, preequalization.**

I. Introduction

BLOCK transmission is commonly used for communicating over dispersive channels affected by intersymbol interference (ISI). The transmitted data stream is parsed into consecutive equal-size blocks and redundancy is added to each block in order to remove interblock interference and devise simple and effective schemes for canceling the ISI. Examples of block transmissions include orthogonal frequency division multiplexing (OFDM) or coded-OFDM (COFDM) systems [25], which have been selected as the standard modulation schemes for audio and video digital terrestrial broadcasting in Europe, and discrete multitone (DMT) transceivers [4], which have been adopted for high bit rate digital subscriber loop (HDSL) and asymmetric digital subscriber loop (ADSL) applications. In particular, when the channel is known at the transmitter, via feedback channels as in HDSL/ADSL applications, the input data stream can be precoded in order to maximize the information rate. An excellent review of precoding for equalization is given in [7]. Multirate precoding for ISI cancellation using filterbanks can also be found in [22]. Indeed, precoding is an old idea dating back to the early works of Harashima [11] and Tomlinson [21], where a "modulo channel inverse" was used as a preequalizer at the transmitter.

However, the main objective in high bit rate transmissions is maximization of the mutual information between transmitter and receiver given performance specifications and limited resources—tasks entailing more than simple mitigation of ISI. Optimality in the sense of maximizing mutual information was proved theoretically for ideal decision feedback equalizers (DFE) in [16], assuming PAM signaling, error-free decisions, and infinite-length feedforward equalizers. An alternative approach is the so-called vector coding (VC), that utilizes a bank of filters whose impulse responses are the eigenvectors of an appropriately defined channel matrix [13]. The VC approach converts size-M block transmission over a frequency-selective channel into transmission over M-parallel independent flat fading channels. DMT and OFDM systems constitute particularly effective implementations of VC, where the transmit/receive filterbanks are substituted by IFFT/FFT blocks, thanks to the introduction of the cyclic prefix which makes the channel eigenvectors equal to the complex exponential filters composing the FFT [4]. Optimality can be reached with these systems asymptotically, as block sizes tend to infinity, by proper allocation of power and number of bits along the subchannels [12].

In spite of the indisputable interest of asymptotic results, it is clearly important from the application point of view to derive systems leading to the maximum mutual information for finite-size block transmissions. Relatively small-size blocks are in fact highly desirable because they avoid excessive decoding delays, storage requirements, and computational load. The optimal scheme for finite block lengths may significantly differ from the asymptotic solution, especially for small-size blocks. Indeed, it was proved in [1] that maximum mutual information with finite-size blocks can be achieved by shaping appropriately the correlation matrix of the transmitted block. However, such an optimum correlation matrix turns out to be non-Toeplitz, and thus spectral pulse shaping based on a linear time-invariant (LTI) filter proposed in [1] can only be approximate, as recognized in [1].

In this work, we prove that the optimal correlation matrix can be induced *exactly*, irrespective of the non-Toeplitz structure of the optimal spectral shaping matrix, using a finite impulse response (FIR) multirate filterbank that introduces

Manuscript received February 1, 1998; revised October 5, 1998. This work was supported under NSF-MIP Grant 9424305.

A. Scaglione and S. Barbarossa are with the Infocom Department, University of Rome "La Sapienza," 00184 Rome, Italy (e-mail: annas@infocom.ing.uniroma1.it; sergio@infocom.ing.uniroma1.it).

G. B. Giannakis was with the Department of Electrical Engineering, University of Virginia, Charlottesville, VA 22903-2442 USA. He is now with the Department of Electrical and Computer Engineering, University of Minnesota, Minneapolis, MN 55455 USA (e-mail: georgios@ece.umn.edu).

Publisher Item Identifier S 0018-9448(99)02080-5.

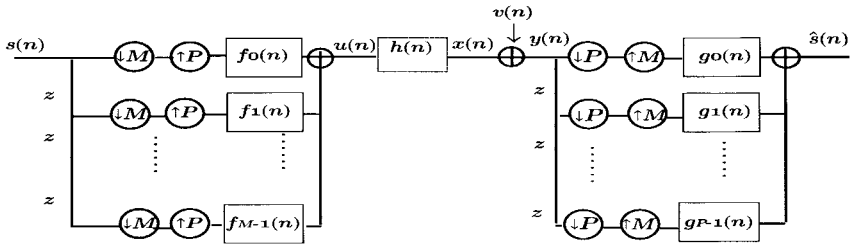

Fig. 1. Multirate discrete-time equivalent transmitter/channel/receiver model.

minimal redundancy on the input bit stream. We adopt the precoding/decoding structure based on multirate filterbanks proposed in [19] and [20] and derive the optimal transmit-receive filterbank pair which maximizes mutual information between transmitter and receiver, subject to a limited transmit-power, for any finite blocklength. The scheme proposed in [20] is particularly appealing in the application at hand because it guarantees existence of blind deterministic methods for channel identification and direct equalization (see also [9]). The optimization herein is performed not only for FIR channels, commonly used in radio communications [17], but also for pole-zero (ARMA) channels which are adopted for parsimonious modeling of copper twisted pair channels encountered in ADSL/HDSL applications [4].

The proposed transceivers convert the frequency-selective channel into M-independent parallel flat fading subchannels—a decomposition reached also by [13] and [14] in the context of line and vector coding. However, our solution stems from maximizing a mutual information criterion and possesses inherent flexibility that yields as special cases zero-forcing (ZF) and minimum mean-square error (MMSE) receivers, *within the class of filterbanks maximizing the information rate*. We also develop power and bit loading strategies aimed at maximizing the information rate, subject to constraints on fixed transmitted power and maximum tolerable bit error rate (BER). To compare with related approaches [13], [18], [24], we also remark on how channel encoding can reduce the signal-to-noise ratio (SNR) margin required to meet a prescribed BER.

The paper is organized as follows. In Section II, we introduce the multirate filterbank transceivers and provide a model for both FIR and ARMA channels, suited for finite block data transmission. The ZF and MMSE filterbank structures maximizing the information rate are derived in Section III. Two power allocation algorithms are developed in Section IV for continuous-amplitude transmissions (infinite granularity of the symbol constellation). Optimal bit allocation, for the more practical case of finite-alphabet constellations, is studied in Section V, where we also compare our method with DMT.

II. Filterbank Transceiver Model

Fig. 1 shows the discrete-time multirate equivalent model of our baseband communication system using filterbank precoders. Successive advancing and downsampling by M per branch creates blocking, or, conversion of the serial data stream $s(n)$ to M-parallel substreams $s_m(n) := s(nM+m)$, where $s_m(n)$ denotes the mth symbol in the nth block of M symbols. Upsamplers by P insert $P-1$ zeros, and the mth upsampler's output is

$$\sum_{i=-\infty}^{\infty} s(iM+m)\delta(n-iP)$$

where $\delta(n)$ denotes Kronecker's delta. With $P > M$, the ratio $(P-M)/P$ represents the amount of redundancy introduced per transmitted block.[1] At the receiver, the rate is reduced by the same amount such that the overall rate remains unchanged. Indicating by $\{f_m(n)\}_{m=0}^{M-1}$ the impulse responses of filters at each branch of the transmit filterbank, our precoder's output is

$$u(n) = \sum_{m=0}^{M-1} \sum_{i=-\infty}^{\infty} s(iM+m) f_m(n-iP). \tag{1}$$

From an input–output (I/O) point of view, our transmit-filterbank precoder takes size-M blocks of $s(n)$, vector filters them, and maps them to size-P blocks of $u(n)$. With $h_c^{(\mathrm{tr})}(t)$ denoting the pulse shaper, we transmit $u_c(t) = \sum_n u(n) h_c^{(\mathrm{tr})}(t-nT)$, where $1/T$ is our transmission rate. After passing through the linear time-invariant (LTI) channel $h_c^{(ch)}(t)$, filtering at the receiver with $h_c^{(rec)}(t)$, and sampling at a rate $1/T$, the received samples in additive Gaussian noise (AGN) $v_c(t)$ are

$$\begin{aligned} y(n) &= \sum_l u(l) h_c((n-l)T) + v_c(nT) \\ &= x(n) + v(n) \\ &= \sum_{l=-\infty}^{\infty} h(l) u(n-l) + v(n) \\ &= \sum_{m=0}^{M-1} \sum_{i=-\infty}^{\infty} s(iM+m) \\ &\quad \cdot \sum_{l=-\infty}^{\infty} h(l) f_m(n-l-iP) + v(n) \end{aligned} \tag{2}$$

where $h(l) := h_c(lT) := (h_c^{(\mathrm{tr})} \star h_c^{(ch)} \star h_c^{(rec)})(lT)$, $\star$ denotes convolution and $v(n) := v_c(nT)$. Similar to channel encoding, but over the complex (as opposed to Galois) field, our redundant precoders expand bandwidth. Specifically, if $1/T_0$ is the symbol rate in $s(n)$, the rate of the transmitted data $u(n)$ is $1/T = (P/M)(1/T_0)$, which implies an excess bandwidth $L/(MT_0)$. However, we do not oversample at the

[1] OFDM and DMT being special cases of filterbank transceivers (e.g., [19]), also introduce redundancy; specifically, $P-M$ corresponds to the length of the so-called cyclic prefix.

receiver, and, hence, contrary to fractionally spaced receivers, there is no need for the pulse shaper to introduce extra excess bandwidth (see also [19] and [20]); i.e., as with OFDM/DMT schemes, $h_c^{(\mathrm{tr})}(t)$ is allowed to have minimum Nyquist bandwidth $1/T$.

A mapping mirror to (1) takes place at the receiver where size-P blocks of $y(n)$ are mapped to size-M blocks of $\hat{s}(n)$ after being filtered through the receive filterbank

$$\hat{s}(n) = \sum_{p=0}^{P-1} \sum_{j=-\infty}^{\infty} y(jP+p) g_p(n-jM). \tag{3}$$

Substituting (2) into (3) leads to a rather cumbersome I/O relationship. However, (1)–(3) can be expressed in compact form using a matrix representation. Denote by $\boldsymbol{s}(n)$ and $\hat{\boldsymbol{s}}(n)$ the $M\times 1$ vectors $\boldsymbol{s}(n) := (s(nM), s(nM+1), \cdots, s(nM+M-1))^T$ and $\hat{\boldsymbol{s}}(n) := (\hat{s}(nM), \hat{s}(nM+1), \cdots, \hat{s}(nM+M-1))^T$, respectively, and by $\boldsymbol{u}(n)$, $\boldsymbol{y}(n)$ the $P\times 1$ vectors $\boldsymbol{u}(n) := (u(nP), u(nP+1), \cdots, u(nP+P-1))^T$ and $\boldsymbol{y}(n) := (y(nP), y(nP+1), \cdots, y(nP+P-1))^T$, respectively. It can be readily verified that (1) and (3) can be cast into the two following equivalent block relationships:

$$\boldsymbol{u}(n) = \sum_{i=-\infty}^{\infty} \boldsymbol{F}_i \boldsymbol{s}(n-i) \tag{4}$$

$$\hat{\boldsymbol{s}}(n) = \sum_{j=-\infty}^{\infty} \boldsymbol{G}_j \boldsymbol{y}(n-j) \tag{5}$$

where $P\times M$ and $M\times P$ matrices $\boldsymbol{F}_i$ and $\boldsymbol{G}_j$ are defined in (6) and (7), given at the bottom of this page. Note that the columns of the ith (jth) matrix $\boldsymbol{F}_i$ ($\boldsymbol{G}_j$) contain the ith (jth) segment of length P (M) of the filters' impulse responses $\{f_m(n)\}_{m=0}^{M-1}$ $\left(\{g_p(n)\}_{p=0}^{P-1}\right)$. An FIR filterbank has filters $\{f_m(n)\}_{m=0}^{M-1}$ $\left(\{g_p(n)\}_{p=0}^{P-1}\right)$ that are FIR, which renders the infinite sums in (1) and (3) finite. In order to generalize our matrix formulation to the LTI-channel I/O relationship, let the $P\times 1$ vector $\boldsymbol{x}(n) := (x(nP), x(nP+1), \cdots, x(nP+P-1))^T$ denote the noise-free block of the channel output and $\boldsymbol{v}(n)$ the corresponding AGN vector with zero-mean and covariance matrix $\boldsymbol{R}_{vv}$, assumed to be full rank. The received data block is then given by

$$\boldsymbol{y}(n) = \boldsymbol{x}(n) + \boldsymbol{v}(n) = \sum_{l=-\infty}^{\infty} \boldsymbol{H}_l \boldsymbol{u}(n-l) + \boldsymbol{v}(n) \tag{8}$$

where the $P\times P$ matrices $\boldsymbol{H}_l$ are defined as

$$\boldsymbol{H}_l := \begin{pmatrix} h(lP) & h(lP-1) & \cdots & h(lP-P+1) \\ h(lP+1) & h(lP) & \ddots & h(lP-P+2) \\ \vdots & \ddots & \ddots & \vdots \\ h(lP+P-1) & h(lP+P-2) & \cdots & h(lP) \end{pmatrix}. \tag{9}$$

Based on (4)–(9), we can write

$$\hat{\boldsymbol{s}}(n) = \sum_{j,\,l,\,i=-\infty}^{\infty} \boldsymbol{G}_j \boldsymbol{H}_l \boldsymbol{F}_i \boldsymbol{s}(n-l-i-j) + \sum_{j=-\infty}^{\infty} \boldsymbol{G}_j \boldsymbol{v}(n-j). \tag{10}$$

The matrix formulation presented so far shows the capability of transmit and receive filterbanks to deal with sequences of vectors as LTI filters do over sequences of samples. It turns out that the transmission scheme in Fig. 1 offers degrees of freedom that can be used effectively to improve system performance. In particular, it is shown in [19] that an FIR filterbank at the receiver can equalize exactly an FIR channel (irrespective of its zero locations) provided that $P > M$.

In the following two sections, we will detail the assumptions on the channel model and filterbank structures adopted in the optimization of our transmission system and point out their consequences on the I/O block relationship (10). We will assume two channel models, which encompass most cases of practical interest in wireless or wired applications: 1) channel with FIR impulse response $h(l)$ [17], where the channel transfer function $H(z) := \mathcal{Z}\{h(l)\}$ is a polynomial of order L and 2) channel with IIR impulse response, modeled as a pole-zero transfer function [4], where $H(z) = B(z)/(1-A(z))$ is a rational function and $B(z)$ and $A(z)$ are polynomials of orders L_B and L_A, respectively. The all-zero FIR model is generally adopted in radio communication channels induced by multipath propagation [17], whereas the pole-zero (ARMA) model offers a parsimonious representation of very long impulse responses in wired transmissions over copper twisted pairs such as those appearing in HDSL/ADSL systems [4].

A. FIR Channel

We adopt the following assumptions.

(a0.1) Channel $h(l)$ is Lth-order FIR with $h(0), h(L) \neq 0$.

(a1.1) (P, M, L) are chosen such that the triplet (P, M, L) satisfies: $P = M + L$, and $M > L$.

$$\boldsymbol{F}_i := \begin{pmatrix} f_0(iP) & f_1(iP) & \cdots & f_{M-1}(iP) \\ f_0(iP+1) & f_1(iP+1) & \cdots & f_{M-1}(iP+1) \\ \vdots & \vdots & \cdots & \vdots \\ f_0(iP+P-1) & f_1(iP+P-1) & \cdots & f_{M-1}(iP+P-1) \end{pmatrix} \tag{6}$$

$$\boldsymbol{G}_j := \begin{pmatrix} g_0(jM) & g_1(jM) & \cdots & g_{P-1}(jM) \\ g_0(jM+1) & g_1(jM+1) & \cdots & g_{P-1}(jM+1) \\ \vdots & \vdots & \cdots & \vdots \\ g_0(jM+M-1) & g_1(jM+M-1) & \cdots & g_{P-1}(jM+M-1) \end{pmatrix} \tag{7}$$

(a2.1) Transmit filters $\{f_m(n)\}_{m=0}^{M-1}$ are of order $<P$, and receive filters $\{g_p(n)\}_{p=0}^{P-1}$ are of order $<M$.

Under (a2.1), we have that $\boldsymbol{F}_i = \boldsymbol{F}_0\delta(i)$ and $\boldsymbol{G}_j = \boldsymbol{G}_0\delta(j)$. Because $P > L$, we infer from (a0.1) that $\boldsymbol{H}_l = \boldsymbol{H}_0\delta(l) + \boldsymbol{H}_1\delta(l-1)$, which together with (a1.1) implies that interblock interference due to the channel entails no more than two successive blocks, namely, $\boldsymbol{s}(n)$ and $\boldsymbol{s}(n-1)$; thus, (10) becomes

$$\hat{\boldsymbol{s}}(n) = \boldsymbol{G}_0\boldsymbol{H}_0\boldsymbol{F}_0\boldsymbol{s}(n) + \boldsymbol{G}_0\boldsymbol{H}_1\boldsymbol{F}_0\boldsymbol{s}(n-1) + \boldsymbol{G}_0\boldsymbol{v}(n) \quad (11)$$

where consistent to definitions (6), (7), and (9), matrix $\boldsymbol{F}_0$ is $P\times M$, $\boldsymbol{G}_0$ is $M\times P$, and $\boldsymbol{H}_0$, $\boldsymbol{H}_1$ are square $P\times P$ matrices.

For perfect, or ZF, reconstruction of $\boldsymbol{s}(n)$ from $\hat{\boldsymbol{s}}(n)$, two options can be pursued [19].

i) Force the last L samples of the transmit filters to be zero, so that $\boldsymbol{F}_0 = (\boldsymbol{F}^T\ \boldsymbol{0})^T$ with $\boldsymbol{F}$ an $M\times M$ matrix and $\boldsymbol{0}$ an $L\times M$ block of zeros, and let $\boldsymbol{G}_0 = \boldsymbol{G}$, where $\boldsymbol{G}$ is a $M\times P$ matrix (we term this option the trailing transmitter zeros approach, or, TZ for short).

ii) Force the first L filters of the receive filterbank to be zero, so that $\boldsymbol{G}_0 = (\boldsymbol{0}\ \ \boldsymbol{G})$, where now $\boldsymbol{G}$ is an $M\times M$ matrix, whereas $\boldsymbol{F}_0 = \boldsymbol{F}$ and $\boldsymbol{F}$ has now dimensionality $P\times M$ (correspondingly, we call this option the leading receiver zeros approach, or, LZ for short).

From an implementation point of view, ii) may be preferred over i) because transmission need not be paused after each block. Although the dimensionalities of $\boldsymbol{F}$ and $\boldsymbol{G}$ will vary for options i) and ii), for brevity we will maintain similar notation for both cases, because if $\boldsymbol{H}$ is defined appropriately, one can adopt a common form for (11)

$$\hat{\boldsymbol{s}}(n) = \boldsymbol{G}\boldsymbol{H}\boldsymbol{F}\boldsymbol{s}(n) + \boldsymbol{G}\boldsymbol{v}(n). \quad (12)$$

Specifically, for case i) of trailing transmitter zeros, $P\times M$ matrix $\boldsymbol{H}$ will be defined as

$$\boldsymbol{H} = \boldsymbol{H}_{\mathrm{TZ}} := \begin{pmatrix} h(0) & 0 & \cdots & 0 \\ \vdots & \ddots & \ddots & \vdots \\ h(L) & \ddots & \ddots & 0 \\ 0 & \ddots & \ddots & h(0) \\ \vdots & \ddots & \ddots & \vdots \\ 0 & \ddots & 0 & h(L), \end{pmatrix} \quad (13)$$

while for case ii) of leading receiver zeros (LZ), $\boldsymbol{H}$ will denote the following $M\times P$ matrix:

$$\boldsymbol{H} = \boldsymbol{H}_{\mathrm{LZ}} := \begin{pmatrix} h(L) & \cdots & h(0) & 0 & \cdots & 0 \\ 0 & \ddots & \ddots & \ddots & \cdots & \vdots \\ \vdots & \vdots & \ddots & \ddots & \ddots & 0 \\ 0 & \cdots & 0 & h(L) & \cdots & h(0) \end{pmatrix}. \quad (14)$$

In [19], ZF equalizing filterbanks are developed even when $P = M+1$ (and $L > 1$), but finite memory is then required in (10) which increases complexity at the receiver. Interestingly, ZF is established in [19] with no statistical assumptions on $s(n)$ and $v(n)$. In this paper, however, we will assume the following.

(a3) Input $\boldsymbol{s}(n)$ and AGN $\boldsymbol{v}(n)$ are generally complex, mutually uncorrelated, stationary with full rank covariance matrices $\boldsymbol{R}_{ss}$ and $\boldsymbol{R}_{vv}$, respectively, ($\sigma_{ss}^2\boldsymbol{I}$ and $\sigma_{vv}^2\boldsymbol{I}$ when white).

Allowing colored inputs accounts for coded transmissions (see, e.g., [14]), while color at the receiver noise incorporates cross-talk, interchannel interference, and residual echo.

B. ARMA Channel

An ARMA channel $h(l)$ is characterized by the rational transfer function

$$\mathcal{Z}\{h(l)\} := H(z) = \frac{B(z)}{1-A(z)} = \frac{\sum_{l=0}^{L_B} b(l)z^{-l}}{1-\sum_{l=0}^{L_A} a(l)z^{-l}} \quad (15)$$

which leads to a scalar I/O relationship $x(n) = \sum_{l=0}^{L_B} b(l)u(n-l) + \sum_{l=0}^{L_A} a(l)x(n-l)$. In our familiar vector-matrix notation, the block version of the latter becomes

$$\boldsymbol{x}(n) = \sum_{l=0}^{N_B} \boldsymbol{B}_l\boldsymbol{u}(n-l) + \sum_{l=0}^{N_A} \boldsymbol{A}_l\boldsymbol{x}(n-l) \quad (16)$$

where $P\times P$ matrices $\boldsymbol{B}_l$ and $\boldsymbol{A}_l$ are defined exactly as $\boldsymbol{H}_l$ in (9), after replacing $h(l)$ by $b(l)$ and $a(l)$, respectively. The summation limits N_B, N_A are functions of M, P, L_B, and L_A. The matrix recursion (16) can be cast in an equivalent vector $\mathcal{Z}$-domain form where block convolutions turn into matrix multiplications, as follows:

$$\begin{aligned}\mathcal{X}(z) &:= \mathcal{Z}\{\boldsymbol{x}(n)\} \\ &= \left(\boldsymbol{I} - \sum_{l=0}^{N_A} \boldsymbol{A}_l z^{-l}\right)^{-1} \left(\sum_{l=0}^{N_B} \boldsymbol{B}_l z^{-l}\right)\mathcal{U}(z) \quad (17)\end{aligned}$$

with $\mathcal{X}(z) := \sum_{n=-\infty}^{\infty} \boldsymbol{x}(n)z^{-n}$ and $\mathcal{U}(z) := \sum_{n=-\infty}^{\infty} \boldsymbol{u}(n)z^{-n}$. Because convolution is commutative, the structure of matrices $\boldsymbol{A}_l$ and $\boldsymbol{B}_l$ is such that the matrix product in (17) commutes as well, hence

$$\begin{aligned}&\left(\boldsymbol{I} - \sum_{l=0}^{N_A} \boldsymbol{A}_l z^{-l}\right)^{-1} \left(\sum_{l=0}^{N_B} \boldsymbol{B}_l z^{-l}\right) \\ &\quad = \left(\sum_{l=0}^{N_B} \boldsymbol{B}_l z^{-l}\right) \left(\boldsymbol{I} - \sum_{l=0}^{N_A} \boldsymbol{A}_l z^{-l}\right)^{-1}. \quad (18)\end{aligned}$$

Our assumptions adopted for ARMA channels are as follows.

(a0.2) Channel $h(l)$ is causal and stable ARMA(L_A,L_B); hence, $b(0)$, $b(L_B) \neq 0$, $a(0)$, $a(L_A) \neq 0$, and the roots of $A(z)$ are inside the unit circle.

(a1.2) (P, M, L) are chosen such that: $P = M + L$, $M > L$ and $L = \max(L_A, L_B)$.

(a2.2) Transmit filters $\{f_m(n)\}_{m=0}^{M-1}$ are of order $<P$, and receive filters $\{g_p(n)\}_{p=0}^{P-1}$ are of order $<M$.

Since (a2.2) coincides with (a2.1), also in this case we have that $\boldsymbol{F}_i = \boldsymbol{F}_0\delta(i)$ and $\boldsymbol{G}_j = \boldsymbol{G}_0\delta(j)$. Moreover, due to (a0.2) and (a1.2), in the block I/O relationships of both $A(z)$ and $B(z)$, interblock interference entails no more than two successive blocks, which means that in (16) we simply have $\boldsymbol{B}_l = \boldsymbol{B}_0\delta(l)+\boldsymbol{B}_1\delta(l-1)$ and $\boldsymbol{A}_l = \boldsymbol{A}_0\delta(l)+\boldsymbol{A}_1\delta(l-1)$. The I/O block relationship of our pole-zero $H(z)$ can be obtained from (17) as

$$\begin{aligned}\mathcal{X}(z) &= \big(\boldsymbol{I}-\boldsymbol{A}_0-\boldsymbol{A}_1z^{-1}\big)^{-1}\big(\boldsymbol{B}_0+\boldsymbol{B}_1z^{-1}\big)\mathcal{U}(z)\\ &= (\boldsymbol{I}-\boldsymbol{A}_0)^{-1}\big(\boldsymbol{I}-\boldsymbol{A}_1(\boldsymbol{I}-\boldsymbol{A}_0)^{-1}z^{-1}\big)^{-1}\\ &\quad\cdot\big(\boldsymbol{B}_0+\boldsymbol{B}_1z^{-1}\big)\mathcal{U}(z)\\ &= (\boldsymbol{I}-\boldsymbol{A}_0)^{-1}\sum_{l=0}^{\infty}\big[\boldsymbol{A}_1(\boldsymbol{I}-\boldsymbol{A}_0)^{-1}\big]^l\\ &\quad\cdot\big(\boldsymbol{B}_0+\boldsymbol{B}_1z^{-1}\big)z^{-l}\mathcal{U}(z)\end{aligned}\tag{19}$$

where in establishing the last equality we used the expansion $(\boldsymbol{I}-\boldsymbol{A}_1(\boldsymbol{I}-\boldsymbol{A}_0)^{-1}z^{-1})^{-1} = \sum_{l=0}^{\infty}[\boldsymbol{A}_1(\boldsymbol{I}-\boldsymbol{A}_0)^{-1}]^l z^{-l}$ which converges because $H(z)$ was assumed stable in (a0.2).

Considering that $\boldsymbol{u}(n) = \boldsymbol{F}_0\boldsymbol{s}(n)$ and inverse $\mathcal{Z}$-transforming (19) implies

$$\begin{aligned}\boldsymbol{x}(n) &= (\boldsymbol{I}-\boldsymbol{A}_0)^{-1}\sum_{l=0}^{\infty}\big[\boldsymbol{A}_1(\boldsymbol{I}-\boldsymbol{A}_0)^{-1}\big]^l\\ &\quad\cdot(\boldsymbol{B}_0\boldsymbol{F}_0\boldsymbol{s}(n-l)+\boldsymbol{B}_1\boldsymbol{F}_0\boldsymbol{s}(n-l-1))\end{aligned}\tag{20}$$

or, equivalently, using (18)

$$\begin{aligned}\boldsymbol{x}(n) &= \boldsymbol{B}_0\sum_{l=0}^{\infty}\big[(\boldsymbol{I}-\boldsymbol{A}_0)^{-1}\boldsymbol{A}_1\big]^l(\boldsymbol{I}-\boldsymbol{A}_0)^{-1}\boldsymbol{F}_0\boldsymbol{s}(n-l)\\ &\quad+\boldsymbol{B}_1\sum_{l=0}^{\infty}\big[(\boldsymbol{I}-\boldsymbol{A}_0)^{-1}\boldsymbol{A}_1\big]^l\\ &\quad\cdot(\boldsymbol{I}-\boldsymbol{A}_0)^{-1}\boldsymbol{F}_0\boldsymbol{s}(n-l-1).\end{aligned}\tag{21}$$

Recalling that $\hat{\boldsymbol{s}}(n) = \boldsymbol{G}_0(\boldsymbol{x}(n)+\boldsymbol{v}(n))$, it will turn out that there are two options to eliminate the infinite memory of the channel due to the AR part in (21).

- Impose on the transmit filterbank the structure $\boldsymbol{F}_0 = (\boldsymbol{I}-\boldsymbol{A}_0)(\boldsymbol{F}^T \;\; \boldsymbol{0})^T$ with $\boldsymbol{F}$ an $M\times M$ matrix and $\boldsymbol{0}$ an $L\times M$ block of zeros, and let $\boldsymbol{G}_0 = \boldsymbol{G}$ where $\boldsymbol{G}$ is an $M\times P$ matrix (TZ approach for ARMA channel).
- Impose on the receive filterbank the structure $\boldsymbol{G}_0 = (\boldsymbol{0} \;\; \boldsymbol{G})(\boldsymbol{I}-\boldsymbol{A}_0)$, where now $\boldsymbol{G}$ is an $M\times M$ matrix whereas $\boldsymbol{F}_0 = \boldsymbol{F}$ and $\boldsymbol{F}$ has now dimensionality $P\times M$ (LZ approach for ARMA channel).

In the TZ case, we first note that according to (a1.2) we have $P > M+L$, which implies that $\boldsymbol{A}_1$ and $\boldsymbol{B}_1$, defined as in (9) with $a(l)$, $b(l)$ replacing $h(l)$, have their first M columns equal to zero. Hence, $\boldsymbol{A}_1(\boldsymbol{F}^T \;\; \boldsymbol{0})^T = \boldsymbol{0}$, and (21) reduces to $\boldsymbol{x}(n) = \boldsymbol{B}_0(\boldsymbol{F}^T \;\; \boldsymbol{0})^T\boldsymbol{s}(n)+\boldsymbol{B}_1(\boldsymbol{F}^T \;\; \boldsymbol{0})^T\boldsymbol{s}(n-1)$. But similar to $\boldsymbol{A}_1$, we have due to (a1.2) that $\boldsymbol{B}_1(\boldsymbol{F}^T \;\; \boldsymbol{0})^T = \boldsymbol{0}$, and the I/O relation becomes

$$\hat{\boldsymbol{s}}(n) = \boldsymbol{G}\boldsymbol{B}_0\big(\boldsymbol{F}^T \;\; \boldsymbol{0}\big)^T\boldsymbol{s}(n)+\boldsymbol{G}\boldsymbol{v}(n) := \boldsymbol{G}\boldsymbol{H}\boldsymbol{F}\boldsymbol{s}(n)+\boldsymbol{G}\boldsymbol{v}(n)\tag{22}$$

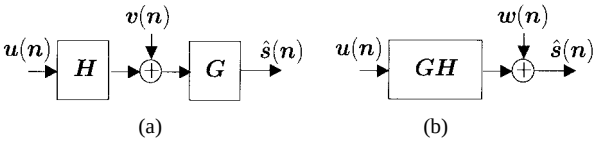

Fig. 2. Matrix equivalent model of Fig. 1.

where $\boldsymbol{H}$ is given by (13), replacing $h(l)$ by $b(l)$. Note that the second equality is simply a definition introduced to establish the parallelism between (22) and (12).

In the LZ case, we invoke again (a1.2) to infer that $(\boldsymbol{0} \;\; \boldsymbol{G})\boldsymbol{B}_1 = (\boldsymbol{0} \;\; \boldsymbol{G})\boldsymbol{A}_1 = \boldsymbol{0}$ and arrive at

$$\begin{aligned}\hat{\boldsymbol{s}}(n) &= (\boldsymbol{0} \;\; \boldsymbol{G})\boldsymbol{B}_0\boldsymbol{F}\boldsymbol{s}(n)+(\boldsymbol{0} \;\; \boldsymbol{G})(\boldsymbol{I}-\boldsymbol{A}_0)\boldsymbol{v}(n)\\ &= \boldsymbol{G}\boldsymbol{H}\boldsymbol{F}\boldsymbol{s}(n)+(\boldsymbol{0} \;\; \boldsymbol{G})(\boldsymbol{I}-\boldsymbol{A}_0)\boldsymbol{v}(n)\end{aligned}\tag{23}$$

where $\boldsymbol{H}$ is given now by (14), replacing $h(l)$ by $b(l)$. Once again, note the similarity between (23) and (12) that will later on facilitate a unifying treatment of FIR and ARMA channels. The dimensionality of the AGN vector $\boldsymbol{v}(n)$ will be $P\times 1$ in both cases.

III. Filterbanks Maximizing Information Rate

In this section, we derive the filterbank pairs maximizing the information rates for transmission over FIR and ARMA channels, separately.

A. Optimal Transceivers for the FIR Channel

Starting with (12), we seek the filterbank pair $(\boldsymbol{F}, \boldsymbol{G})$ that for given $\boldsymbol{H}$, $\boldsymbol{R}_{ss}$, and $\boldsymbol{R}_{vv}$ maximizes the possible information rate, subject to a limited average transmitted power.

Fig. 2(a) is the block (or matrix) counterpart of Fig. 1 under all assumptions leading to (12), namely, (a0.1)–(a2.1) with TZ or LZ filterbanks, while Fig. 2(b) is equivalent to Fig. 2(a) if one defines $\boldsymbol{T} := \boldsymbol{G}\boldsymbol{H}$ and $\boldsymbol{w}(n) := \boldsymbol{G}\boldsymbol{v}(n)$. Vector $\boldsymbol{u}(n)$ is our channel's block input, and $\hat{\boldsymbol{s}}(n) = \boldsymbol{T}\boldsymbol{u}(n)+\boldsymbol{w}(n)$ denotes the received block. The starting point in maximizing the information rate is to express the mutual information between channel input $\boldsymbol{u}(n)$ and receive-filterbank output $\hat{\boldsymbol{s}}(n)$ as a function of matrices $\boldsymbol{F}$ and $\boldsymbol{G}$. We will borrow a result derived in [1, Thm. 1], and state it without proof in a slightly more general form that allows for colored input and noise vectors.

Lemma 1: Consider the finite-dimensional vector model $\hat{\boldsymbol{s}} = \boldsymbol{T}\boldsymbol{u}+\boldsymbol{w}$, where $\boldsymbol{u}$ and $\boldsymbol{w}$ are zero-mean independent vectors with covariance matrices $\boldsymbol{R}_{uu}$ and $\boldsymbol{R}_{ww}$ and $\boldsymbol{w}$ is (generally complex and circularly) Gaussian. The normalized (per input symbol) mutual information, $I(\boldsymbol{u};\hat{\boldsymbol{s}})$, between any block $\boldsymbol{u}$ of P channel input symbols and the corresponding block $\hat{\boldsymbol{s}}$ of M receiver output symbols is maximized when $\boldsymbol{u}$ is Gaussian, and is given by[2]

$$I(\boldsymbol{u};\hat{\boldsymbol{s}}) = \frac{1}{P}\log_2\Big|\Big(\boldsymbol{R}_{uu}^{\dagger}+\boldsymbol{T}^H\boldsymbol{R}_{ww}^{-1}\boldsymbol{T}\Big)\boldsymbol{R}_{uu}\Big|.\tag{24}$$

[2]We adopt hereafter the following notation: $|\boldsymbol{A}|$ denotes the determinant of $\boldsymbol{A}$, the superscript H denotes transposition and conjugation, and † denotes pseudoinverse.

The matrix $(\boldsymbol{R}_{uu}^{\dagger}+\boldsymbol{T}^H\boldsymbol{R}_{ww}^{-1}\boldsymbol{T})\boldsymbol{R}_{uu}$ may be rank deficient and, in such a case, as in the evaluation of the entropy of Gaussian random vectors having a singular covariance matrix, the determinant has to be substituted by the product of the nonzero singular values of $(\boldsymbol{R}_{uu}^{\dagger}+\boldsymbol{T}^H\boldsymbol{R}_{ww}^{-1}\boldsymbol{T})\boldsymbol{R}_{uu}$ [1, Appendix II].

As expected intuitively, spectral shaping of the transmitted blocks [described by $\boldsymbol{R}_{uu}$ in (24)] affects mutual information and thus capacity and information rate of our block transmission through the channel. Without specifying the receiver structure and assuming AWGN, the mutual information $I(\boldsymbol{u};\boldsymbol{y})$ was maximized in [1] with respect to $\boldsymbol{R}_{uu}$. The optimum $\boldsymbol{R}_{uu}$ was found to be non-Toeplitz, which corresponds to a nonstationary $u(n)$ and indicates that the desired spectral shaper must be time-varying since $s(n)$ is stationary. LTI lattice structures were proposed in [1] to *approximate* the desired time-varying transmitter.

The spectral shaper in our setup is the transmit filterbank $\boldsymbol{F}$ which induces the linear periodically varying I/O relationship (1). Surprisingly, $\boldsymbol{F}$ will turn out to offer the *exact* spectral shaper leading to the optimum $\boldsymbol{R}_{uu}$ sought by [1]. Along with the optimum $\boldsymbol{G}$, the optimum $\boldsymbol{F}$ will be derived in closed form as a result of maximizing (24) and will thus achieve the maximum information rate for block transmissions.

Our optimization result is summarized in the following (see Appendix for the proof).

Theorem 1: Suppose (a0.1)–(a2.1) and (a3) hold true, and let the transmit power $\mathcal{P}_0:=\mathrm{tr}(\boldsymbol{F}\boldsymbol{R}_{ss}\boldsymbol{F}^H)$, channel matrix $\boldsymbol{H}$ in (13) or (14), the input symbol covariance matrix $\boldsymbol{R}_{ss}$ and the noise covariance matrix $\boldsymbol{R}_{vv}$, be given. Denoting by $\boldsymbol{U}$, $\boldsymbol{V}$ the unitary matrices, and by $\boldsymbol{\Delta}$, $\boldsymbol{\Lambda}$ the diagonal matrices resulting from the eigen decompositions

$$\boldsymbol{R}_{ss}=\boldsymbol{U}\boldsymbol{\Delta}\boldsymbol{U}^H,\qquad \boldsymbol{H}^H\boldsymbol{R}_{vv}^{-1}\boldsymbol{H}=\boldsymbol{V}\boldsymbol{\Lambda}\boldsymbol{V}^H \tag{25}$$

the optimum $(\boldsymbol{F},\boldsymbol{G})$ filterbank pair maximizing (24) is given by[3]

$$\boldsymbol{F}_{opt}=\boldsymbol{V}\boldsymbol{\Phi}\boldsymbol{U}^H,\qquad \boldsymbol{G}_{opt}=\boldsymbol{U}\boldsymbol{\Gamma}\boldsymbol{\Lambda}^{-1}\boldsymbol{V}^H\boldsymbol{H}^H\boldsymbol{R}_{vv}^{-1} \tag{26}$$

where $\boldsymbol{\Gamma}$ denotes an arbitrary invertible matrix and $\boldsymbol{\Phi}$ is a diagonal matrix with entries

$$\phi_{ii}=\sqrt{\max\left(\frac{\mathcal{P}_0+\mathrm{tr}\,(\boldsymbol{\Lambda}^{-1})}{M\delta_{ii}}-\frac{1}{\lambda_{ii}\,\delta_{ii}},0\right)} \tag{27}$$

and $\lambda_{ii}(\delta_{ii})$ is the ith diagonal entry of $\boldsymbol{\Lambda}(\boldsymbol{\Delta})$. □

First, let us interpret Theorem 1 with special cases. If $s(n)$ is white with unit variance, then $\boldsymbol{R}_{ss}=\boldsymbol{I}$ and $\boldsymbol{F}_{opt}=\boldsymbol{V}\boldsymbol{\Phi}$. In such a case, the impulse response of the ith transmit filter is $\boldsymbol{f}_{i,opt}=\phi_{ii}\boldsymbol{v}_i$, where $\boldsymbol{v}_i$ is the ith column of $\boldsymbol{V}$, and thus $|\phi_{ii}|^2$ represents the power assigned to the ith filter (recall that matrix $\boldsymbol{\Phi}$ is diagonal). If $\boldsymbol{v}(n)$ is white, $\boldsymbol{R}_{vv}=\sigma_{vv}^2\boldsymbol{I}$ and $\boldsymbol{v}_i$ in (25) corresponds to the ith eigenvector of the channel matrix $\boldsymbol{H}^H\boldsymbol{H}$.

Note that the optimum pair $(\boldsymbol{F}_{opt},\boldsymbol{G}_{opt})$ is nonunique, and matrix $\boldsymbol{\Gamma}$ in (26) offers degrees of freedom which can be exploited to satisfy added requirements. For example, judicious selections of $\boldsymbol{\Gamma}$ yield the ZF or the minimum mean-square error (MMSE) receive filterbank, as testified by the following corollaries.

Corollary 1: Under (a0.1)–(a3), the ZF receiver filterbank that maximizes mutual information in (24) under fixed transmitted power $\mathcal{P}_0$, is obtained by setting $\boldsymbol{\Gamma}=\boldsymbol{\Phi}^{\dagger}$. The corresponding receive-filterbank matrix is

$$\boldsymbol{G}_{opt}^{zf}=\left(\boldsymbol{R}_{vv}^{-1/2}\boldsymbol{H}\boldsymbol{F}_{opt}\right)^{\dagger}\boldsymbol{R}_{vv}^{-1/2}. \tag{28}$$

Proof: Recalling (12), the ZF condition requires that $\boldsymbol{G}\boldsymbol{H}\boldsymbol{F}=\boldsymbol{I}$. From (25) and (26), we obtain

$$\boldsymbol{G}\boldsymbol{H}\boldsymbol{F}=\boldsymbol{U}\boldsymbol{\Gamma}\boldsymbol{\Lambda}^{-1}\boldsymbol{V}^H\boldsymbol{H}^H\boldsymbol{R}_{vv}^{-1}\boldsymbol{H}\boldsymbol{V}\boldsymbol{\Phi}\boldsymbol{U}^H=\boldsymbol{U}\boldsymbol{\Gamma}\boldsymbol{\Phi}\boldsymbol{U}^H. \tag{29}$$

Therefore, the choice $\boldsymbol{\Gamma}_{zf}=\boldsymbol{\Phi}^{\dagger}$ leads to the ZF solution. Substituting $\boldsymbol{\Gamma}_{zf}$ into (26) yields (28). □

Corollary 2: Under (a0.1)–(a3), the MMSE receiver filterbank that maximizes mutual information in (24) under fixed transmitted power $\mathcal{P}_0$, is obtained by setting $\boldsymbol{\Gamma}_{\mathrm{mmse}}=\boldsymbol{\Delta}\boldsymbol{\Phi}^H(\boldsymbol{\Lambda}^{-1}+\boldsymbol{\Phi}^H\boldsymbol{\Delta}\boldsymbol{\Phi})^{-1}$. The corresponding receive-filterbank matrix is

$$\boldsymbol{G}_{opt}^{\mathrm{mmse}}=\boldsymbol{R}_{ss}\boldsymbol{F}^H\boldsymbol{H}^H\left(\boldsymbol{R}_{vv}+\boldsymbol{H}\boldsymbol{F}_{opt}\boldsymbol{R}_{ss}\boldsymbol{F}_{opt}^H\boldsymbol{H}^H\right)^{-1}. \tag{30}$$

Proof: Using (12), the MSE $\mathcal{E}:=\mathrm{tr}\{E([\hat{\boldsymbol{s}}(n)-\boldsymbol{s}(n)][\hat{\boldsymbol{s}}(n)-\boldsymbol{s}(n)]^H)\}$ can be decomposed into a residual ISI term plus an output noise power term as follows:

$$\mathcal{E}=\mathrm{tr}\left((\boldsymbol{G}\boldsymbol{H}\boldsymbol{F}-\boldsymbol{I})\boldsymbol{R}_{ss}(\boldsymbol{G}\boldsymbol{H}\boldsymbol{F}-\boldsymbol{I})^H\right)+\mathrm{tr}\left(\boldsymbol{G}\boldsymbol{R}_{vv}\boldsymbol{G}^H\right) \tag{31}$$

where $\mathrm{tr}\,(\boldsymbol{T})$ indicates the trace of matrix $\boldsymbol{T}$. Substituting (26) into (31), we find

$$\mathcal{E}=\mathrm{tr}\left((\boldsymbol{\Gamma}\boldsymbol{\Phi}-\boldsymbol{I})\boldsymbol{\Delta}(\boldsymbol{\Gamma}\boldsymbol{\Phi}-\boldsymbol{I})^H\right)+\mathrm{tr}\left(\boldsymbol{\Gamma}\boldsymbol{\Lambda}^{-1}\boldsymbol{\Gamma}^H\right) \tag{32}$$

and the matrix $\boldsymbol{\Gamma}_{\mathrm{mmse}}$ minimizing (32) can be found by equating to zero the gradient of (32) with respect to $\boldsymbol{\Gamma}$

$$\boldsymbol{\Gamma}_{\mathrm{mmse}}=\boldsymbol{\Delta}\boldsymbol{\Phi}^H\left(\boldsymbol{\Lambda}^{-1}+\boldsymbol{\Phi}^H\boldsymbol{\Delta}\boldsymbol{\Phi}\right)^{-1}. \tag{33}$$

The corresponding receive filterbank matrix is given by (30). □

Without optimizing information rate, jointly optimal MMSE transceivers of multiinput–multioutput systems under fixed transmit power have been derived also in [23]. The IIR frequency-domain designs of [23] are optimized via iterative minimization of Lagrange multipliers. In contrast, our MMSE designs of Corollary 2 lead to closed-form FIR filterbanks within the class of transceivers maximizing information rate.

Further insight is gained on our optimal transceivers from Fig. 3, where cascaded matrices implement the $\boldsymbol{F}_{opt}$ and $\boldsymbol{G}_{opt}$ filterbanks of (26). If $\overline{\boldsymbol{s}}(n):=\boldsymbol{U}^H\boldsymbol{s}(n)$ denotes the $\boldsymbol{U}^H$ block output, it follows easily from (25) that $\boldsymbol{R}_{\overline{s}\,\overline{s}}=\boldsymbol{\Delta}$, i.e., components $\overline{s}_i(n)$ are mutually uncorrelated and each with variance $\sigma_{\overline{s}_i\,\overline{s}_i}^2=\delta_{ii}$. Hence, the block $\boldsymbol{U}^H$ decorrelates the entries of our (possibly colored) input vector $\boldsymbol{s}(n)$. The next diagonal block $\boldsymbol{\Phi}$ can be decomposed as [cf. (27)] $\boldsymbol{\Phi}=\boldsymbol{D}_{\phi}\boldsymbol{\Delta}^{-1/2}$, where $\boldsymbol{D}_{\phi}$ depends only on $\mathcal{P}_0$ and $\boldsymbol{\Lambda}$.

[3] In the LZ case, matrix $\boldsymbol{H}^H\boldsymbol{R}_{vv}^{-1}\boldsymbol{H}$ in (25) is rank deficient, and $\boldsymbol{\Lambda}$ has to be slightly modified [see (70) in the Appendix].

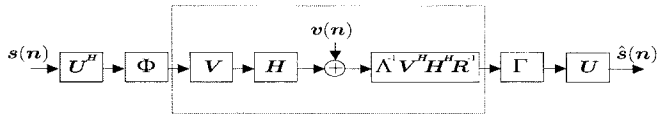

Fig. 3. Optimal filterbank transceivers: matrix model.

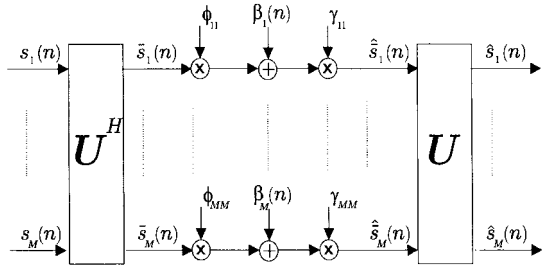

Fig. 4. Parallel channel equivalent of Fig. 3.

With the decomposition $\boldsymbol{\Phi U}^H = \boldsymbol{D}_\phi(\boldsymbol{\Delta}^{-1/2}\boldsymbol{U}^H)$, we identify that the first part of our transmit filterbank $\boldsymbol{F}_{opt}$, performs prewhitening, while the second part, namely, $\boldsymbol{VD}_\phi$, tunes the transmit filters according to the eigenstructure of the propagation channel which depends on the ISI matrix and the AGN covariance $\boldsymbol{R}_{vv}$ [cf. (25)]. When the AGN is white, $\boldsymbol{V}$ in (25) is formed by the left singular vectors of the channel matrix $\boldsymbol{H}$ (or the eigenvectors of $\boldsymbol{H}^H\boldsymbol{H}$) and the corresponding part of the precoder filterbank, $\boldsymbol{VD}_\phi$ is composed of nothing, but transmit filters each with impulse response $\boldsymbol{v}_i$ (the ith column of $\boldsymbol{V}$) and gain $d_{\phi_{ii}} := \phi_{ii}\sqrt{\delta_{ii}}$ as suggested by (27).

Consider now the multichannel equivalent of the cascaded matrix systems inside the box of Fig. 3. Using (25), we find that its vector transfer function is

$$\boldsymbol{\Lambda}^{-1}\boldsymbol{V}^H\boldsymbol{H}^H\boldsymbol{R}_{vv}^{-1}\boldsymbol{HV} = \boldsymbol{\Lambda}^{-1}\boldsymbol{V}^H\boldsymbol{V\Lambda V}^H\boldsymbol{V} = \boldsymbol{I} \tag{34}$$

which implies that if we select a diagonal $\boldsymbol{\Gamma}$, the matrix (or block) channel between the outer blocks $\boldsymbol{U}^H$ and $\boldsymbol{U}$ is described by the diagonal matrix $\boldsymbol{\Gamma\Phi}$. Hence, the M subchannels are decoupled and Fig. 3 becomes equivalent to Fig. 4 which depicts also the flat fading on each of the parallel subchannels as the multiplicative factors $\phi_{ii}\,\gamma_{ii}$ corresponding to the diagonal elements of $\boldsymbol{\Gamma\Phi}$. To establish statistical (in addition to deterministic) channel decoupling, we consider the transformed noise $\boldsymbol{\beta}(n) := \boldsymbol{\Lambda}^{-1}\boldsymbol{V}^H\boldsymbol{H}^H\boldsymbol{R}_{vv}^{-1}\boldsymbol{v}(n)$ at the output of the block in Fig. 3. Using again (25), the covariance matrix of $\boldsymbol{\beta}(n)$ is

$$\boldsymbol{R}_{\beta\beta} = \boldsymbol{\Lambda}^{-1}\boldsymbol{V}^H\boldsymbol{H}^H\boldsymbol{R}_{vv}^{-1}\boldsymbol{R}_{vv}\boldsymbol{R}_{vv}^{-1}\boldsymbol{HV\Lambda}^{-1} = \boldsymbol{\Lambda}^{-1} \tag{35}$$

justifying the decorrelation and thus independence [since $\boldsymbol{\beta}(n)$ is AGN] among the subchannels. We have thus established that.

Corollary 3: With $\boldsymbol{\Gamma}$ diagonal, the mutual information maximizing filterbank transceivers of Theorem 1 render the block transmission ISI channel model equivalent to M-independent parallel ISI-free subchannels each with flat fading gains $\phi_{ii}\gamma_{ii}$ and uncorrelated AGN samples $\beta_i(n)$ with variance $1/\lambda_{ii}$; i.e.,

$$\hat{\overline{s}}_i(n) = \phi_{ii}\,\gamma_{ii}\,\overline{s}_i(n) + \gamma_{ii}\,\beta_i(n). \tag{36}$$

Because $\overline{s}_i(n)$ has variance δ_{ii}, the SNR_i at the output of the ith subchannel is

$$\mathrm{SNR}_i = \frac{\delta_{ii}|\phi_{ii}|^2|\gamma_{ii}|^2}{\lambda_{ii}^{-1}|\gamma_{ii}|^2} = \delta_{ii}|\phi_{ii}|^2\lambda_{ii}. \tag{37}$$

The independence of the parallel subchannels asserted in Corollary 3 implies a corresponding decomposition of the maximum mutual information in (24) as [see also (59) in the Appendix]

$$\begin{aligned} I(\boldsymbol{u};\,\hat{\boldsymbol{s}}) &= \frac{1}{P}\sum_{i=1}^{M}\log_2(1+\lambda_{ii}\delta_{ii}|\phi_{ii}|^2) \\ &= \frac{1}{P}\sum_{i=1}^{M}\log_2(1+\mathrm{SNR}_i) \end{aligned} \tag{38}$$

with ϕ_{ii} given by (27). Interestingly, the SNR_i and $I(\boldsymbol{u};\,\hat{\boldsymbol{s}})$ do not depend on the matrix $\boldsymbol{\Gamma}$, which can thus be selected according to Corollaries 1 or 2, without affecting the maximum information rate.

As the block length $M \to \infty$, the energy per subchannel suggested by (27) corresponds to the well-known "water-pouring" (or "water-filling") principle (see, e.g., [8, ch. 8]), which under *ideal* DFE *conditions* (correct decisions entering the feedback loop) was reached also by [14] in the context of finite length block codes. Note though that in contrast to our FIR filterbank transceivers, the ideal ZF-DFE entails IIR feedforward filtering. Trailing transmitter zeros and transmit filters corresponding to eigenvectors of the channel matrix were also derived in [13] relying on a ZF/constrained power criterion for white input and noise processes. In this work, in addition to treating more general TZ/LZ cases, for both FIR and ARMA channels, we derived the optimal filterbanks by directly maximizing the information rate and obtained the ZF and MMSE receivers, within the class of filterbanks maximizing the information rate.

Example 1: An example of application is reported in Fig. 5, dealing with block ($P = 64$) transmission over a frequency-selective channel characterized by an FIR filter with zeros at 0.9, $0.9j$, $-0.9j$, in the presence of additive white Gaussian noise $v_{\mathrm{AGN}}(n)$ at SNR $= 10$ dB, plus stationary Gaussian narrowband interference $v_{\mathrm{NBI}}(n)$, generated to be independent of $v_{\mathrm{AGN}}(n)$. With $v(n) := v_{\mathrm{AGN}}(n) + v_{\mathrm{NBI}}(n)$, we applied Theorem 1 to obtain our transmit filters $\{f_m(n)\}_{m=0}^{M-1}$ from the columns of $\boldsymbol{F}_{opt}$ in (26).

Fig. 5 shows the normalized channel transfer function $|H(f)|/|H(0)|$ (dotted line), the interference spectral density (solid line), and the average of the optimal filter magnitudes $M^{-1}\sum_{m=0}^{M-1}|F_m(f)|$ (dashed line). As expected, the optimal filters do not allocate any power at the frequency bin containing the interference and allocate most of the power in the frequencies where the channel gain (SNR) is higher, as predicted by the water-filling principle [8].

B. Optimal Transceivers for the ARMA Channel

Instead of (12), our starting equations for pole-zero channels are (22) and (23) for the TZ and LZ cases, respectively.

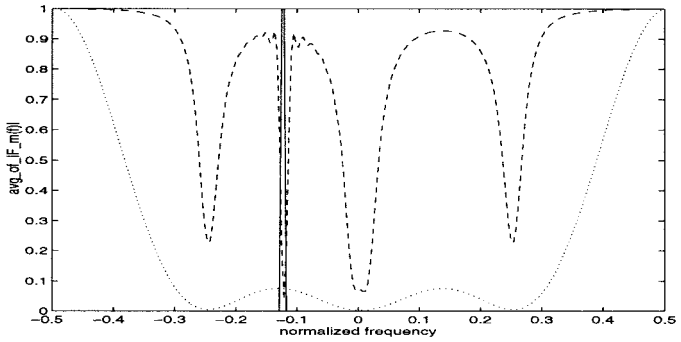

Fig. 5. Average of the optimal transmit filters transfer functions (dashed line), channel transfer function (dotted line), and interference (solid line).

Proceeding similar to the FIR-channel case, we have the equivalent channel model of Fig. 2(b) by setting $\boldsymbol{w}(n) := \boldsymbol{G}\boldsymbol{v}(n)$ in the TZ case and $\boldsymbol{w}(n) = (\boldsymbol{0}\ \ \boldsymbol{G})(\boldsymbol{I} - \boldsymbol{A}_0)\boldsymbol{v}(n)$ in the LZ case. As a consequence, Lemma 1, whose derivation relied on (12) for FIR channels, applies also to ARMA channels provided that $\boldsymbol{T} := \boldsymbol{G}\boldsymbol{H}$ and $\boldsymbol{R}_{ww} := E\{\boldsymbol{w}(n)\boldsymbol{w}^H(n)\}$ are defined according to the modifications pointed out in Section II-B concerning the TZ and LZ cases. However, the TZ structure does not lead to an optimal transmit filterbank because the argument of the determinant in (24) cannot be diagonalized as with FIR channels (see also Appendix). On the contrary, as we will see next, the optimal transceivers can be reached using the LZ scheme, by extending the formulation derived for the FIR channel to the ARMA case. The parallelism between (12) and (23) allows us to establish directly the counterpart of Theorem 1 for pole-zero channels.

Theorem 2: Suppose (a0.2)–(a2.2) and (a3) hold true and let the transmit power $\mathcal{P}_0 := \mathrm{tr}\,(\boldsymbol{F}\boldsymbol{R}_{ss}\boldsymbol{F}^H)$, ARMA channel [with matrix $\boldsymbol{H}$ in (14) having $b(l)$ instead of $h(l)$], the input symbol covariance matrix $\boldsymbol{R}_{ss}$, and the noise covariance matrix $\boldsymbol{R}_{vv}$ be given. Denoting by $\boldsymbol{U}, \boldsymbol{V}$ the unitary matrices, and by $\boldsymbol{\Delta}$, $\boldsymbol{\Lambda}$ the diagonal matrices resulting from the eigen decompositions

$$\begin{aligned} \boldsymbol{R}_{ss} &= \boldsymbol{U}\boldsymbol{\Delta}\boldsymbol{U}^H \\ \boldsymbol{H}^H(\boldsymbol{I} - \boldsymbol{A}_0)^{-H}\boldsymbol{R}_{vv}^{-1}(\boldsymbol{I} - \boldsymbol{A}_0)^{-1}\boldsymbol{H} &= \boldsymbol{V}\boldsymbol{\Lambda}\boldsymbol{V}^H \end{aligned} \tag{39}$$

the optimum $(\boldsymbol{F}, \boldsymbol{G})$ filterbank pair maximizing (24) is given by

$$\begin{aligned} \boldsymbol{F}_{opt} &= \boldsymbol{V}\boldsymbol{\Phi}\boldsymbol{U}^H \\ \boldsymbol{G}_{opt} &= \boldsymbol{U}\boldsymbol{\Gamma}\boldsymbol{\Lambda}^{-1}\boldsymbol{V}^H\boldsymbol{H}^H(\boldsymbol{I} - \boldsymbol{A}_0)^{-H}\boldsymbol{R}_{vv}^{-1}(\boldsymbol{I} - \boldsymbol{A}_0)^{-1} \end{aligned} \tag{40}$$

with $\boldsymbol{\Gamma}$ and $\boldsymbol{\Phi}$ as in Theorem 1, and as per Section II-B, $\boldsymbol{F}_0 = \boldsymbol{F}_{opt}$ and $\boldsymbol{G}_0 = (\boldsymbol{0}\ \ \boldsymbol{G}_{opt})(\boldsymbol{I} - \boldsymbol{A}_0)$.

All remarks made in Section III-A apply also to the ARMA case. In particular, applying Corollaries 1 and 2, matrix $\boldsymbol{\Gamma}$ can be chosen to yield the ZF or MMSE equalizing filterbanks for pole-zero channels. It is interesting to observe that the factor $(\boldsymbol{I} - \boldsymbol{A}_0)$ in $\boldsymbol{G}_0$ means that the receiver equalizes the AR part first and thus converts the IIR channel into an FIR channel and then proceeds as if the channel is FIR (see also [4] for related remarks).

IV. Optimal Power Allocation

The multichannel setup summarized in Corollary 3 and Fig. 4 shows that the optimal filterbank pair in Theorem 1 offers the finite blocklength counterpart of the familiar result of optimal power allocation on a set of $M \to \infty$ independent Gaussian channels (see [6, pp. 250–252]). As with infinite subchannels, some of the low-SNR subchannels have to be excluded from our finite blocklength transmission as well. Indeed, when some of the $|\phi_{ii}|^2$ in (27) are zero, the corresponding ith subchannel will not be used. Excluding some subchannels implies a different power distribution (loading) across the usable subchannels $\overline{M} \leq M$ (see, e.g., [5] and references therein). The goal of loading algorithms is to allocate power and bits across the subchannels in order to maximize the information rate, under the constraints of fixed average transmit power and an upper bounded bit error rate. The final information rate will thus be affected not only by pulse shaping, but also through the power and bit allocation schemes.

In this section, we concentrate on optimal power allocation, assuming the optimal filterbank of Theorem 1 and ignoring discretization effects due to $s(n)$ constellations belonging to a finite alphabet. So, we initially assume the ideal condition of infinite granularity [continuous-amplitude $s(n)$], and postpone the bit allocation issue for the ensuing section. Two power loading algorithms are described next.

A. Power Loading Algorithm #1

Let $\overline{M}$ denote the number of nonzero ϕ_{ii}'s in (27). Using $\boldsymbol{R}_{ss}$ and $\boldsymbol{F}$ from (25) and (26), we can write the transmit power constraint as

$$\mathrm{tr}\,\left(\boldsymbol{F}\boldsymbol{R}_{ss}\boldsymbol{F}^H\right) = \sum_{i=1}^{\overline{M}} \delta_{ii}|\phi_{ii}|^2 = \mathcal{P}_0. \tag{41}$$

The $\overline{M}$ subchannels effectively used must satisfy $\phi_{ii} > 0$, $\forall\, i \in [1, \overline{M}]$, and because $\delta_{ii} > 0\ \forall i$, we infer from (27) that $\overline{M}$ must obey the inequality

$$\overline{M} \max_{i=1,\cdots,\overline{M}}(1/\lambda_{ii}) - \sum_{k=1}^{\overline{M}} 1/\lambda_{kk} \leq \mathcal{P}_0. \tag{42}$$

Since $\mathcal{P}_0 > 0$, there exists a value $\overline{M} \geq 1$ which satisfies (42). Such a value of $\overline{M}$ guarantees that

$$|\phi_{ii}|^2 = \frac{\mathcal{P}_0 + \displaystyle\sum_{k=1}^{\overline{M}} \frac{1}{\lambda_{kk}}}{\delta_{ii}\overline{M}} - \frac{1}{\delta_{ii}\lambda_{ii}} > 0, \qquad \forall\, i = 1, \cdots, \overline{M} \tag{43}$$

and thus (41) holds true as well. With $\overline{M}$ replacing M, the maximum information rate changes correspondingly to [cf. (38) and (43)]

$$\overline{I}(\boldsymbol{u};\, \hat{\boldsymbol{s}}) = \frac{1}{P}\sum_{i=1}^{\overline{M}} \log_2\left(\frac{\mathcal{P}_0 + \displaystyle\sum_{k=1}^{\overline{M}} \frac{1}{\lambda_{kk}}}{\overline{M}}\,\lambda_{ii}\right) \tag{44}$$

and the redundancy added to each block is now $(P-\overline{M})/P$.

The loading algorithm resulting from (42) and (43) is the following:

1) Compute δ_{ii}'s and λ_{ii}'s from (25) and sort λ_{ii}'s in ascending order.
2) Set $\overline{M} = M$.
3) While $\overline{M}\max_{i=1,\ldots,\overline{M}}(1/\lambda_{ii}) - \sum_{k=1}^{\overline{M}} 1/\lambda_{kk} > \mathcal{P}_0$, set $\overline{M} = \overline{M} - 1$.
4) Allocate power according to

$$|\phi_{ii}|^2 = \frac{\mathcal{P}_0 + \sum_{k=1}^{\overline{M}} \frac{1}{\lambda_{kk}}}{\delta_{ii}\overline{M}} - \frac{1}{\delta_{ii}\lambda_{ii}}.$$

To obviate low-SNR ("weaker") subchannels, this section's loading strategy is to discard, if necessary, transmit-filterbank branches and redistribute power to "stronger" subchannels while adhering to the fixed power $\mathcal{P}_0$. An alternative strategy that does not discard, but rather "rescales" filterbank branches is described in the next section.

B. Power Loading Algorithm #2

Let us introduce a real positive parameter α to alter our loadings to

$$|\phi_{ii}^{\alpha}|^2 = \frac{\mathcal{P}_0 + \frac{1}{\alpha}\sum_{k=1}^{M} \frac{1}{\lambda_{kk}}}{\delta_{ii}M} - \frac{1}{\alpha\delta_{ii}\lambda_{ii}}. \tag{45}$$

By summing (45) over $i = 1, \cdots, M$, it is straightforward to verify that the power constraint (41) is automatically satisfied, for any $\alpha > 0$. We wish to select an α which guarantees that $|\phi_{ii}|^2 > 0$, $\forall i \in [1, M]$. From (27), we deduce that if

$$M \max_i (1/\lambda_{ii}) - \sum_{k=1}^{M} 1/\lambda_{kk} \leq \mathcal{P}_0 \tag{46}$$

then $|\phi_{ii}|^2 > 0\ \forall i \in [1, M]$, in which case we simply take $\alpha = 1$ and allocate power optimally according to (27). However, if (46) is not satisfied, we set

$$\alpha = \frac{M \max_i(1/\lambda_{ii}) - \sum_{k=1}^{M} 1/\lambda_{kk}}{\mathcal{P}_0} \tag{47}$$

and "rescale" the $|\phi_{ii}|^2$'s using (45). The loading algorithm follows these steps.

1) Compute δ_{ii}'s and λ_{ii}'s from (25) and sort λ_{ii}'s in ascending order.
2) Set

$$\alpha = \max\left[\frac{M \max_i(1/\lambda_{ii}) - \sum_{k=1}^{M} 1/\lambda_{kk}}{\mathcal{P}_0}, 1\right].$$

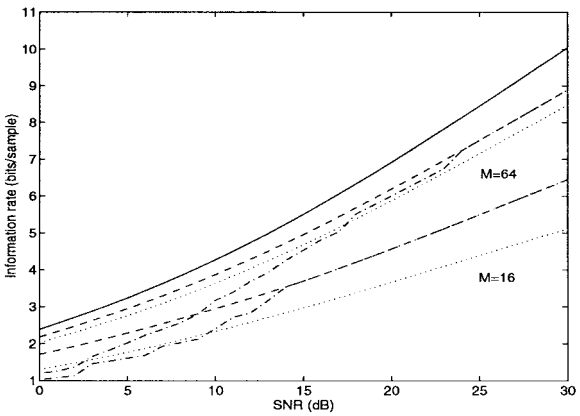

Fig. 6. Channel capacity (solid line) and information rates, in bits per sample, achieved with optimal filterbank, loading algorithm #1 (dashed-dotted line) and #2 (dashed line), and with DMT (dotted line), using two different block lengths M.

3) Allocate power according to

$$|\phi_{ii}^{\alpha}|^2 = \frac{\mathcal{P}_0 + \frac{1}{\alpha}\sum_{k=1}^{M} \frac{1}{\lambda_{kk}}}{\delta_{ii}M} - \frac{1}{\alpha\delta_{ii}\lambda_{ii}}.$$

The number of subchannels effectively used here is $\geq\overline{M}$ found with the first loading algorithm and the power distribution is consequently different.

Let us now compare the information rates achievable with the two loading algorithms and with DMT when both $s(n)$ and $v(n)$ are white with $\boldsymbol{R}_{ss} = \boldsymbol{I}$ and $\boldsymbol{R}_{vv} = \sigma_n^2\boldsymbol{I}$. We compute the information rate pertaining to DMT using (24), with $\boldsymbol{R}_{uu} = \boldsymbol{F}\boldsymbol{F}^H$, $\boldsymbol{T} = \boldsymbol{G}\boldsymbol{H}$, $\boldsymbol{R}_{ww} = \boldsymbol{G}\boldsymbol{R}_{vv}\boldsymbol{G}^H$, and using a $P \times M$ precoding matrix $\boldsymbol{F}$, whose columns are complex exponentials, $f_m(l) = \exp(j2\pi ml/M)$, $l = 0, \cdots, P-1$, with cyclic prefix $L = P - M$ [4]. Also in this case, as with (24), the determinant is computed as the product of the nonzero singular values of the matrix $(\boldsymbol{R}_{uu}^{\dagger} + \boldsymbol{T}^H\boldsymbol{R}_{ww}^{-1}\boldsymbol{T})\boldsymbol{R}_{uu}$. If some singular values are less than one, thus implying a negative contribution to the information rate, the most severely faded subchannel is discarded and the power is equally redistributed on the remaining channels; the procedure is iterated until all the singular values are greater than one [4].

Example 2: The comparison reported in Fig. 6, is based on an FIR channel of order $L = 5$, with zeros at $0.9, \pm 0.9j, \exp(\pm j\pi/4)$, using two block sizes $M = 16$ and $M = 64$. The figure shows the channel capacity (solid line) computed as in [8, p. 388], and the information rates (in bits per sample) achievable with DMT (dotted line) and with the loading algorithms #1 (dashed-dotted line) and #2 (dashed line). From Fig. 6, we observe that the information rates achievable with DMT and with the optimal filters tend to coincide and approach closely the channel capacity as the block size increases, but the optimal filterbank outperforms DMT. The asymptotic (as $M \to \infty$) convergence of the two is justified because the complex exponentials used for DMT filters coincide with the channel eigenvectors, arising from the filterbank optimization of Theorem 1. For relatively large blocks, the suboptimality of DMT is compensated by the

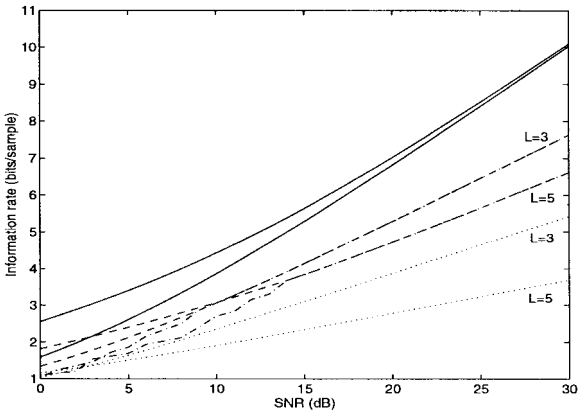

Fig. 7. Channel capacity (solid line) and information rates, in bits per sample, achieved with optimal filterbank, loading algorithm #1 (dashed-dotted line) and #2 (dashed line), and with DMT (dotted line), relative to two channels having $L = 3$ and $L = 5$ zeros on the unit circle ($M = 32$).

computational advantage it has over the optimal filterbank because the former is FFT based while the latter requires eigen decompositions of large matrices. Conversely, when small-size blocks are used, the added flexibility gained with the optimal filters relative to complex exponentials is helpful to approach the theoretical information rate more closely.

The relative improvement achieved with the optimal filters over the DMT increases also as the channel's frequency selectivity increases. As an example, Fig. 7 shows the information rates obtained with the optimal filterbank and with DMT, using blocks of size $M = 32$, for transmissions over two kinds of channels: one with $L = 3$ zeros at $1, \pm j$ and the other with $L = 5$ zeros at $1, \pm j, \pm\exp(j\pi/4)$. From Fig. 7, we observe that the advantage of using the optimal filterbank is more pronounced as the number of zeros on the unit circle increases. In fact, when channel zeros are uniformly spaced on the unit circle, DMT avoids transmission over the corresponding subchannels and distributes the available power on the remaining channels. In contrast, depending on the channel's eigen characteristics, the optimal approach reshapes all the transmit filters and this extra flexibility offers the aforementioned improvement over the DMT.

In a nutshell, we deduce that: 1) both optimal and DMT schemes allow reliable transmission at information rates approaching channel capacity, as the block size increases; 2) the optimal filterbank offers advantages with respect to DMT, which are more evident for small block sizes and highly selective channels; and 3) loading algorithm #2 outperforms loading algorithm #1.

V. Optimal Bit Allocation Subject to Symbol Error Rate Bound

In communications practice, one of the main parameters characterizing quality of service is the maximum tolerable BER. In this section, we show how to allocate power and bits across the subchannels in order to guarantee a prescribed upper bound on the BER, under the constraint of fixed average transmit power. In the previous section, we computed the optimal power distribution across the subchannels, without accounting for the fact that $s(n)$ comes from a finite alphabet (infinite granularity). Here, we consider the practical case where information bits are mapped onto constellations of finite size. With reference to Fig. 4, the number of bits b_i on the ith subchannel characterized by SNR_i could be, in principle, set equal to its capacity limit $b_i = \log_2(1+\mathrm{SNR}_i)$. However, this choice may not necessarily guarantee the desired bound on the BER. Similar to the loading algorithm proposed in [5] for DMT transceivers, we introduce an SNR margin ξ [relative to what is required by (38) to maximize $I(\boldsymbol{u};\hat{\boldsymbol{s}})$], such that the choice

$$b_i = \log_2\left(1 + \frac{\mathrm{SNR}_i}{\xi}\right) \tag{48}$$

adheres to the BER requirement. In the next section, we will show how to reduce this margin by channel encoding our information sequence.

We describe next how to allocate the bits over the M subchannels in order to have on each subchannel an error probability less than or equal to a given maximum value $P_{e,\max}$. Toward this goal, we have to specify a constellation for each subchannel i, and we choose to focus on QAM, with corresponding order Q_i. As per Corollary 3, the output of the ith subchannel will be ISI free, and the error probability $P_e^{(i)}$ can be upper bounded using known results for Q_i-QAM transmissions over AGN channels (see, e.g., [3, p. 225])

$$\begin{aligned} P_e^{(i)} &< 2\mathrm{erfc}\left(\sqrt{\frac{3\mathcal{E}_s}{2N_0(Q_i-1)}}\right) \\ &= 2\mathrm{erfc}\left(\sqrt{\frac{3\delta_{ii}\lambda_{ii}|\phi_{ii}|^2}{2(Q_i-1)}}\right) \\ &= 2\mathrm{erfc}\left(\sqrt{\frac{3\lambda_{ii}\left(\mathcal{P}_0 + \sum_{k=1}^{\overline{M}} \lambda_{kk}^{-1}\right) - 3}{2(Q_i-1)}}\right) \\ &:= P_{e,\max}^{(i)} \end{aligned} \tag{49}$$

where $\mathcal{E}_s$ is the symbol energy, N_0 is the one-sided noise power spectral density, and for the equalities we used (37) and (27), respectively. The bound $P_{e,\max}^{(i)}$ in (49) implies a corresponding bound on Q_i and thus in the number of bits $b_i := \log_2 Q_i$. Upon inverting the erfc function in (49), the latter can be found as

$$\begin{aligned} b_{i,\max} &= \log_2\left(1 + \frac{\delta_{ii}\lambda_{ii}|\phi_{ii}|^2}{\xi}\right) \\ &= \log_2\left(1 + \frac{\lambda_{ii}\left(\mathcal{P}_0 + \sum_{k=1}^{\overline{M}} \lambda_{kk}^{-1}\right) - 1}{\xi}\right) \end{aligned} \tag{50}$$

with

$$\xi := (2/3)\left[\mathrm{erfc}^{-1}\left(P_{e,\max}^{(i)}/2\right)\right]^2. \tag{51}$$

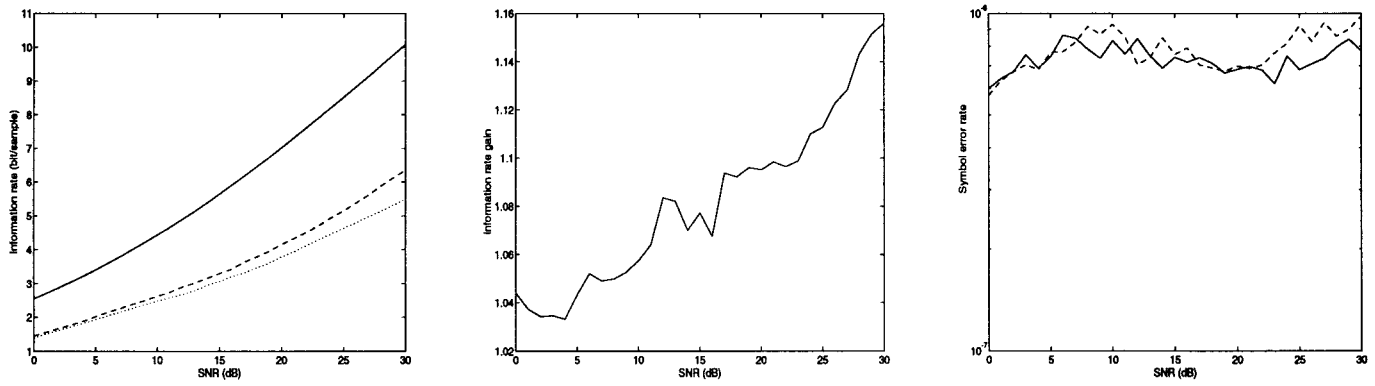

(a) (b) (c)

Fig. 8. Results pertaining to channel 1: (a) channel capacity (solid line) and information rates (bits/sample) achieved with our method (dashed line) and with DMT (dotted line); (b) gain in information rate achieved with our method with respect to DMT; and (c) symbol error probability for DMT (dashed) and this paper's method (solid).

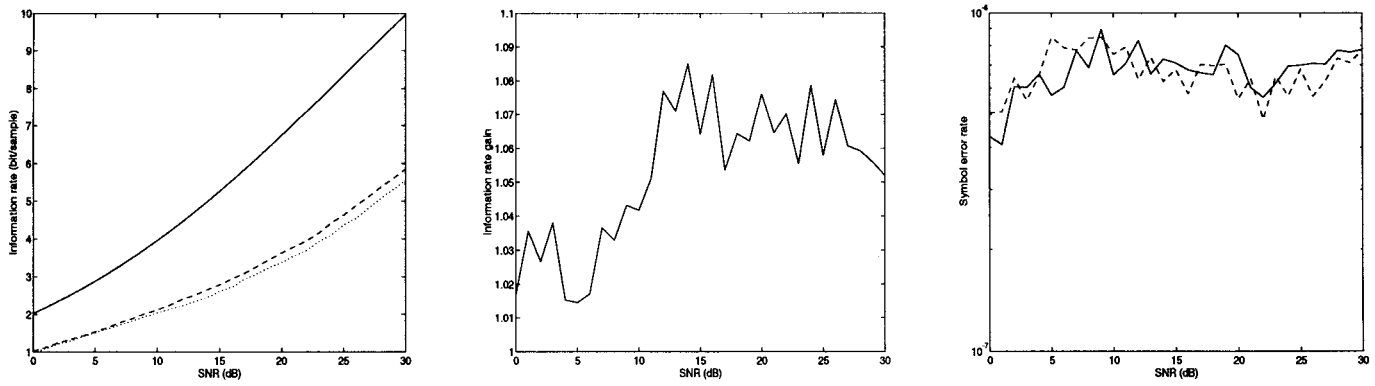

(a) (b) (c)

Fig. 9. Results pertaining to channel 2: (a) channel capacity (solid line) and information rates (bps) achieved with our method (dashed line) and with DMT (dotted line); (b) gain in information rate achieved with our method with respect to DMT; and (c) symbol error probability for DMT (dashed) and this paper's method (solid).

Since the number of bits b_i cannot be smaller than one, we obtain from (50) the equivalent inequality

$$|\phi_{ii}|^2 \geq \frac{\xi}{\lambda_{ii}\delta_{ii}}. \tag{52}$$

Condition (52) increases the lower bound of the possible values of $|\phi_{ii}|^2$, relative to the zero lower bound in (27). Dropping the max operator from (27), the number $\hat{M}$ of subchannels actually used changes accordingly and must be such that [cf. (52)]

$$|\phi_{ii}|^2 = \frac{1}{\hat{M}\delta_{ii}}\left(\mathcal{P}_0 + \sum_{k=1}^{\hat{M}} \frac{1}{\lambda_{kk}}\right) - \frac{1}{\lambda_{ii}\delta_{ii}} \geq \frac{\xi}{\lambda_{ii}\delta_{ii}} \tag{53}$$

where (53) is assured if

$$\frac{1}{\hat{M}}\left(\mathcal{P}_0 + \sum_{k=1}^{\hat{M}} \frac{1}{\lambda_k}\right) \geq \max_i \left(\frac{\xi+1}{\lambda_i}\right). \tag{54}$$

Equations (50) and (54) are important in practice because they provide guidelines for optimal bit allocation per subchannel and the number of usable subchannels so that the upper bound on the symbol error rate is not exceeded. Note that we have relied on the bound rather than the equality sign in (49) because the latter leads to a smaller (and thus more conservative choice for the) constellation size. Although the aggregate probability of error is the target, similar to existing loading algorithms (see, e.g., [4]), using the per-subchannel bound in (49) guarantees error probabilities less than or equal to the prescribed BER.

We have compared this section's bit allocation scheme using the optimal filterbank in (26) versus the DMT that employs the FFT based filterbank. The DMT was implemented with cyclic prefix and with a number of bits on the ith subchannel chosen as in (48) with $\text{SNR}_i = |H(i/M)|^2\mathcal{P}_0/\hat{M}$, where $H(f)$ denotes the channel transfer function and $\mathcal{P}_0$ is the transmitted power, which is equally distributed across the effectively used $\hat{M}$ subchannels.

Example 3: Figs. 8 and 9 show theoretical curves pertaining to transmission with block length $M = 16$ over two channels having different frequency selectivity: channel 1 has zeros at $[1, \pm j, \exp(\pm j\pi/4)]$ and channel 2 has zeros at $[0.8, \pm 0.8j, 0.8\exp(\pm j\pi/4)]$. The desired bound on the error rate is $P_{e,\max} = 10^{-6}$. Each figure shows: 1) the information rate achieved with our method (dashed line) and DMT (dotted line), together with the channel capacity (solid line); 2) the ratio between the information rates achieved using our method

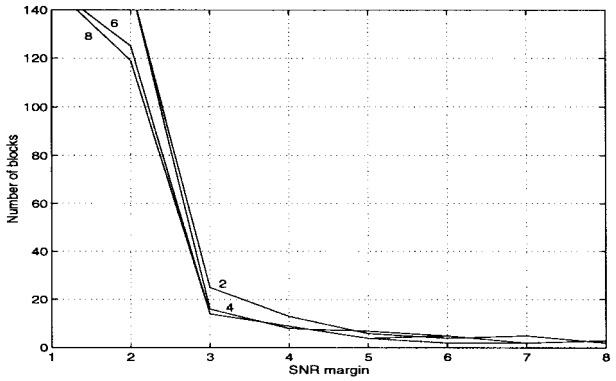

Fig. 10. Number of blocks as a function of the SNR margin $\xi(N)$ for different number of bits.

and DMT; and 3) the symbol error rate achieved with the two methods. The variability of the curves in 3) is due to the finite-alphabet of the transmitted symbols which makes it impossible to achieve the requirement on the prescribed BER exactly.

From Figs. 8 and 9, we infer that the gain of the optimal approach with respect to DMT can be as high as 15%, and is more evident when the channel selectivity increases.

Remark: Because coding allows b_i to be rational, SNR margin ξ in (51) can be reduced by channel encoding each subchannel separately (cf. [13], [18], and [24] where coding is applied across subchannels). Using Reed–Solomon (RS) for the ith subchannel, we can express BER before ($:= P_{s_i}$) and after $[P_{s_i}^{(\mathrm{RS})}]$ decoding as $P_{s_i} \approx [P_{s_i}^{(\mathrm{RS})} t!(n_i - t - 1)!/(n_i - 1)!]^{1/(t+1)}$, where (k_i) n_i is the number of (un)coded bits over N blocks, $t_i := \lfloor (n_i - k_i)/2 \rfloor$ denotes the number of correctable bits, and the approximation holds for $P_{s_i} \ll (t+1)/(n-t-1)$; see also [17, p. 430]. With Gray encoding, information rate $b_i(N) := \log_2(1 + \mathrm{SNR}_i/\xi(N))$, bit rate $c_i(N) := n_i/N$, and imposing the quality of service (QoS) BER bound on $P_{s_i}^{(\mathrm{RS})}$, we can determine the pair $(\xi(N), N)$ that satisfies (with minimum N to reduce decoding delays)

$$\left[P_{s_i}^{(\mathrm{RS})} \frac{t!(n_i - t - 1)!}{(n_i - 1)!}\right]^{1/(t+1)} < \frac{2}{c_i(N)} \mathrm{erfc}\left(\sqrt{\frac{3(2^{b_i(N)} - 1)}{2(2^{c_i(N)} - 1)} \xi(N)}\right)$$

and compare it with $\xi(1) := \xi$ in (51) in order to quantify the gain in SNR margin using the ratio $\xi(1)/\xi(N)$. With $b_i(N) = 6$, $c_i(N) = 7$, and QoS BER $= 10^{-6}$, the uncoded transmission requires $\xi(1) = 8.42$. For $b_i(N) = 2, 4, 6, 8$, Fig. 10 shows that, e.g., by RS coding over 20 blocks, one can accommodate a dynamic range of two–eight bits, with an SNR margin $\xi(N) = 3$ instead of $\xi(1) = 8.42$.

VI. Conclusions and Discussion

In this paper, we proposed multirate filterbank transceivers guaranteeing block data transmission at the maximum information rate, subject to a fixed average transmit power, for both FIR and IIR (pole-zero) channels. Within the class of filters maximizing the information rate, the inherent flexibility of the proposed structure was exploited to derive ZF and minimum mean-square error receive filterbanks. The proposed transceivers outperform DMT for small-size blocks transmitted through highly frequency-selective channels, at the expense of added complexity required to perform (non-FFT-based) eigen decomposition.

Transmission at the maximum information rate in general does not meet the constraint on the bit error rate, which has to be lower than a prescribed upper bound dictated by the required quality of service, unless ideal infinite memory coding is applied. Using a finite-size code memory, it is necessary to introduce an SNR margin in the computation of the bit distribution along the subchannels. In this paper, we proposed two power and bit loading algorithms satisfying the bit error rate requirement and showed how the SNR margin can be reduced by resorting to coding. Works are in progress to develop decision-feedback filterbank transceivers and extend the proposed approach to time-varying transmission channels. In fact, the multirate filterbank approach may be particularly useful for imposing transmit-correlation matrices with non-Toeplitz structures.

Similar to existing precoding schemes, in deriving our optimal filterbank transceivers we assumed that the transmission channel is known. In applications such as ADSL/HDSL and cable television, feedback loops provide channel information from the receiver to the transmitter. However, information may be imperfect due to channel estimation errors and presence of time-varying interference such as near-end cross talk (NEXT) or far-end cross talk (FEXT). Therefore, it is important to analyze how sensitive the performance of proposed transceivers is to imperfect channel knowledge. Recalling that our transceivers are obtained from the eigenvectors of the channel matrix, we expect sensitivity to depend upon the channel's frequency-selectivity. From the perturbation theory of matrix eigen decompositions [10, Sec. 7.2], we also expect that the sensitivity increases when the channel matrix $\boldsymbol{H}^H \boldsymbol{R}_{vv}^{-1} \boldsymbol{H}$ tends to have multiple eigenvalues. In such cases, large errors may result when computing channel matrix eigenvectors corresponding to (even approximately) equal eigenvalues. In practice, this situation arises when dealing with mildly frequency-selective channels whose smallest eigenvalues tend to become nearly equal to zero. On the other hand, the loading strategy prevents transmission on those "weak" (high-attenuation) subchannels. Summarizing, although one expects "sensitive estimates" of transmit filters corresponding to small eigenvalues, using the bit allocation strategy described herein, only minimal (or even zero) information is going to be transmitted on those "sensitive" subchannels. Intuitively speaking, the overall strategy based on maximizing the information rate seems to be robust with respect to small perturbations of the channel response. Thorough analysis of the sensitivity problem in the context of block transmission schemes goes beyond the scope of this paper and deserves deeper investigation.

Appendix
Proof of Theorem 1

Hadamard's inequality [6, p. 502] implies that $I(\boldsymbol{u}; \hat{\boldsymbol{s}})$ is maximized when the matrix $(\boldsymbol{R}_{uu}^{\dagger} + \boldsymbol{T}^H \boldsymbol{R}_{ww}^{-1} \boldsymbol{T}) \boldsymbol{R}_{uu}$ is

diagonal. We will prove that the pair (26) achieves this diagonalization for both the TZ and the LZ cases.

TZ Case: Recalling that $\boldsymbol{u}(n) = \boldsymbol{F}\boldsymbol{s}(n)$, $\boldsymbol{T} = \boldsymbol{G}\boldsymbol{H}$, $\boldsymbol{w}(n) = \boldsymbol{G}\boldsymbol{v}(n)$, and using (26) and (25), we have

$$\boldsymbol{R}_{uu} = \boldsymbol{F}\boldsymbol{R}_{ss}\boldsymbol{F}^H = \boldsymbol{V}\boldsymbol{\Phi}\boldsymbol{\Delta}\boldsymbol{\Phi}^H\boldsymbol{V}^H \tag{55}$$

$$\boldsymbol{G}\boldsymbol{H} = \boldsymbol{U}\boldsymbol{\Gamma}\boldsymbol{\Lambda}^{-1}\boldsymbol{V}^H\boldsymbol{H}^H\boldsymbol{R}_{vv}^{-1}\boldsymbol{H} = \boldsymbol{U}\boldsymbol{\Gamma}\boldsymbol{V}^H \tag{56}$$

$$\boldsymbol{R}_{ww} = \boldsymbol{G}\boldsymbol{R}_{vv}\boldsymbol{G}^H = \boldsymbol{U}\boldsymbol{\Gamma}\boldsymbol{\Lambda}^{-1}\boldsymbol{\Gamma}^H\boldsymbol{U}^H \tag{57}$$

$$\boldsymbol{T}^H\boldsymbol{R}_{ww}^{-1}\boldsymbol{T} = \boldsymbol{V}\boldsymbol{\Gamma}^H\boldsymbol{U}^H\left(\boldsymbol{U}\boldsymbol{\Gamma}\boldsymbol{\Lambda}^{-1}\boldsymbol{\Gamma}^H\boldsymbol{U}^H\right)^{-1}\boldsymbol{U}\boldsymbol{\Gamma}\boldsymbol{V}^H = \boldsymbol{V}\boldsymbol{\Lambda}\boldsymbol{V}^H. \tag{58}$$

Substituting these expressions into (24), we obtain

$$\begin{aligned} I(\boldsymbol{u};\,\hat{\boldsymbol{s}}) &= \frac{1}{P}\log_2\left|\boldsymbol{I} + \boldsymbol{V}\boldsymbol{\Lambda}\boldsymbol{V}^H\boldsymbol{V}\boldsymbol{\Phi}\boldsymbol{\Delta}\boldsymbol{\Phi}^H\boldsymbol{V}^H\right| \\ &= \frac{1}{P}\log_2\left|\boldsymbol{I} + \boldsymbol{\Lambda}\boldsymbol{\Phi}\boldsymbol{\Delta}\boldsymbol{\Phi}^H\right|. \end{aligned} \tag{59}$$

Notice that (59) does not depend on $\boldsymbol{\Gamma}$, so that the only assumption about $\boldsymbol{\Gamma}$, used to simplify (58), is that it has to be invertible. We seek the matrix $\boldsymbol{\Phi}$ which maximizes $I(\boldsymbol{u};\,\hat{\boldsymbol{s}})$, under the constraint of finite transmit power

$$tr\left(\boldsymbol{F}\boldsymbol{R}_{ss}\boldsymbol{F}^H\right) = tr\left(\boldsymbol{\Phi}\boldsymbol{\Delta}\boldsymbol{\Phi}^H\right) = \mathcal{P}_0. \tag{60}$$

According to Hadamard's inequality, matrix $\boldsymbol{\Lambda}\boldsymbol{\Phi}\boldsymbol{\Delta}\boldsymbol{\Phi}^H$ must be diagonal, and since $\boldsymbol{\Lambda}$ is diagonal we infer that $\boldsymbol{\Phi}\boldsymbol{\Delta}\boldsymbol{\Phi}^H$ has to be diagonal. We will argue the following.

Lemma: Without loss of generality (w.l.o.g.) $\boldsymbol{\Phi}$ can be considered as diagonal matrix.

Because $\boldsymbol{\Delta}$ is diagonal, the product $\boldsymbol{\Phi}\boldsymbol{\Delta}\boldsymbol{\Phi}^H$ which has to be diagonal, must have diagonal entries given by

$$\left(\boldsymbol{\Phi}\boldsymbol{\Delta}\boldsymbol{\Phi}^H\right)_{ii} = \sum_{j=1}^{M}\delta_{jj}|\phi_{ij}|^2. \tag{61}$$

If $\boldsymbol{\Phi}$ in (61) maximizes (59) subject to (60), so does the diagonal matrix $\hat{\boldsymbol{\Phi}}$ with entries such that

$$\delta_{ii}|\hat{\phi}_{ii}|^2 = \sum_{j=1}^{M}\delta_{jj}|\phi_{ij}|^2. \tag{62}$$

Comparing (61) with (62), proves that assuming $\boldsymbol{\Phi}$ diagonal imposes no restrictions on the optimization. □

According to the Lemma, taking $\boldsymbol{\Phi}$ to be diagonal simplifies (59) and (60) to

$$I(\boldsymbol{u};\,\hat{\boldsymbol{s}}) = \frac{1}{P}\sum_{i=1}^{M}\log_2(1 + \lambda_{ii}\delta_{ii}|\phi_{ii}|^2) \tag{63}$$

$$\text{tr}\left(\boldsymbol{F}\boldsymbol{R}_{ss}\boldsymbol{F}^H\right) = \sum_{i=1}^{M}\delta_{ii}|\phi_{ii}|^2 = \mathcal{P}_0. \tag{64}$$

Therefore, the optimal entries ϕ_{ii} can be found by maximizing the Lagrangian

$$\begin{aligned} L(|\phi_{ii}|^2,\,\mu) = \frac{1}{P}\sum_{i=1}^{M}\log_2(1 + \lambda_{ii}\delta_{ii}|\phi_{ii}|^2) \\ - \mu\left(\sum_{i=1}^{M}\delta_{ii}|\phi_{ii}|^2 - \mathcal{P}_0\right). \end{aligned} \tag{65}$$

Equating partial derivatives of the Lagrangian with respect to $|\phi_{ii}|^2$ to zero, we find

$$\frac{\partial L(|\phi_{ii}|^2,\mu)}{\partial|\phi_{ii}|^2} = \frac{1}{P}\log_2(e)\,\frac{\lambda_{ii}\delta_{ii}}{1 + \lambda_{ii}\delta_{ii}|\phi_{ii}|^2} - \mu\delta_{ii} = 0. \tag{66}$$

Hence, we obtain

$$|\phi_{ii}|^2 = \frac{\log_2(e)}{\mu P\delta_{ii}} - \frac{1}{\lambda_{ii}\delta_{ii}}. \tag{67}$$

Imposing the power constraint, we can find μ as

$$\mu = \frac{(M/P)\log_2(e)}{\mathcal{P}_0 + \text{tr}\,(\boldsymbol{\Lambda}^{-1})}. \tag{68}$$

Therefore, the optimal matrix $\boldsymbol{\Phi}$ has diagonal entries

$$|\phi_{ii}|^2 = \max\left(\frac{\mathcal{P}_0 + \text{tr}\,(\boldsymbol{\Lambda}^{-1})}{M\delta_{ii}} - \frac{1}{\lambda_{ii}\delta_{ii}},\,0\right) \tag{69}$$

and this completes the proof for the TZ case.

LZ Case: For the LZ case we will maintain the same notation as before, but now $\boldsymbol{V}$ is the $P\times M$ matrix whose columns are the eigenvectors associated to the nonzero eigenvalues of the $P\times P$ matrix $\boldsymbol{H}^H\boldsymbol{R}_{vv}^{-1}\boldsymbol{H}$, which is rank deficient because in the LZ case $\boldsymbol{H}$ is $M\times P$ and $\boldsymbol{R}_{vv}$ is $M\times M$. Hence, we can write

$$\boldsymbol{H}^H\boldsymbol{R}_{vv}^{-1}\boldsymbol{H} = \overline{\boldsymbol{V}}\begin{pmatrix}\boldsymbol{\Lambda} & \boldsymbol{0}\\ \boldsymbol{0} & \boldsymbol{0}\end{pmatrix}\overline{\boldsymbol{V}}^H \tag{70}$$

where $\boldsymbol{V}$ contains the first M columns of the $P\times P$ unitary matrix $\overline{\boldsymbol{V}}$; i.e., the eigenvectors associated to the $M\times M$ matrix $\boldsymbol{\Lambda}$. Proceeding similar to the TZ case, (56)–(58) change now to

$$\boldsymbol{G}\boldsymbol{H} = \boldsymbol{U}(\boldsymbol{\Gamma}\ \boldsymbol{0})\boldsymbol{V}^H \tag{71}$$

$$\boldsymbol{R}_{ww} = \boldsymbol{U}\boldsymbol{\Gamma}\boldsymbol{\Lambda}^{-1}\boldsymbol{\Gamma}^H\boldsymbol{U}^H \tag{72}$$

$$\boldsymbol{T}^H\boldsymbol{R}_{ww}^{-1}\boldsymbol{T} = \overline{\boldsymbol{V}}\begin{pmatrix}\boldsymbol{\Lambda} & \boldsymbol{0}\\ \boldsymbol{0} & \boldsymbol{0}\end{pmatrix}\overline{\boldsymbol{V}}^H \tag{73}$$

where we have used

$$\boldsymbol{V}^H\overline{\boldsymbol{V}} = (\boldsymbol{I}_{M\times M}\,\boldsymbol{0}_{M\times L}). \tag{74}$$

Once again, substituting (71)–(73) into (24) we obtain

$$I(\boldsymbol{u};\,\hat{\boldsymbol{s}}) = \frac{1}{P}\log_2\left|\begin{pmatrix}\boldsymbol{I} & \boldsymbol{0}\\ \boldsymbol{0} & \boldsymbol{0}\end{pmatrix} + \overline{\boldsymbol{V}}\begin{pmatrix}\boldsymbol{\Lambda}\boldsymbol{\Phi}\boldsymbol{\Delta}\boldsymbol{\Phi}^H & \boldsymbol{0}\\ \boldsymbol{0} & \boldsymbol{0}\end{pmatrix}\overline{\boldsymbol{V}}^H\right|. \tag{75}$$

The matrix in the argument of the determinant is singular and this poses a problem in evaluating $I(\boldsymbol{u};\,\hat{\boldsymbol{s}})$. However, this problem is in principle the same as the one showing up in the entropy derivation of a Gaussian random vector having a singular covariance matrix, and the solution was given in [1, Appendix II]. In particular, applying the result proved in [1] to our case, we infer that the determinant must be replaced by the product of the nonzero eigenvalues. Thus, assuming $\boldsymbol{\Phi}$ to be diagonal and applying the same arguments as in the TZ case, (75) becomes

$$I(\boldsymbol{u};\,\hat{\boldsymbol{s}}) = \frac{1}{P}\sum_{i=1}^{M}\log_2(1 + \lambda_{ii}\delta_{ii}|\phi_{ii}|^2). \tag{76}$$

It is important to remark that the final expression (75) coincides with (59), so that the optimization of $\boldsymbol{\Phi}$ is carried out exactly as in the TZ case. □

REFERENCES

[1] N. Al-Dhahir and J. M. Cioffi, "Block transmission over dispersive channels: Transmit filter optimization and realization, and MMSE-DFE receiver performance," *IEEE Trans. Inform. Theory*, vol. 42, pp. 137–160, Jan. 1996.

[2] M. Barton and M. L. Honig, "Optimization of discrete multitone to maintain spectrum compatibility with other transmission systems on twisted copper pairs," *IEEE J. Select. Areas Commun.*, pp. 1558–1563, Dec. 1995.

[3] S. Benedetto, E. Biglieri, and V. Castellani, *Digital Transmission Theory*. Englewood Cliffs, NJ: Prentice-Hall, 1987.

[4] J. S. Chow, J. C. Tu, and J. M. Cioffi, "A discrete multitone transceiver system for HDSL applications," *IEEE J. Select. Areas Commun.*, pp. 895–908, Aug. 1991.

[5] P. S. Chow, J. M. Cioffi, and J. A. C. Bingham, "A practical discrete multitone transceiver loading algorithm for data transmission over spectrally shaped channels," *IEEE Trans. Commun.*, pp. 773–775, Mar. 1995.

[6] T. M. Cover and J. A. Thomas, *Elements of Information Theory*. New York: Wiley, 1991.

[7] G. D. Forney, Jr. and M. V. Eyuboğlu, "Combined equalization and coding using precoding," *IEEE Commun. Mag.*, pp. 25–34, Dec. 1991.

[8] R. Gallager, *Elements of Information Theory*. New York: Wiley, 1968.

[9] G. B. Giannakis, "Filterbanks for blind channel identification and equalization," *IEEE Signal Processing Lett.*, vol. 4, pp. 184–187, June 1997.

[10] G. H. Golub and C. F. Van Loan, *Matrix Computations*. Baltimore, MD: Johns Hopkins Univ. Press, 1989.

[11] H. Harashima and H. Miyakawa, "Matched-transmission technique for channels with intersymbol interference," *IEEE Trans. Commun.*, pp. 774–780, Aug. 1972.

[12] I. Kalet, "The multitone channel," *IEEE Trans. Commun.*, vol. 37, pp. 119–124, Feb. 1989.

[13] S. Kasturia, J. T. Aslanis, and J. M. Cioffi, "Vector coding for partial response channels," *IEEE Trans. Inform. Theory*, vol. 36, pp. 741–761, July 1990.

[14] J. W. Lechleider, "The optimum combination of block codes and receivers for arbitrary channels," *IEEE Trans. Commun.*, pp. 615–621, May 1990.

[15] I. Lee, J. S. Chow, and J. M. Cioffi, "Performance evaluation of a fast computation algorithm for the DMT in high-speed subscriber loop," *IEEE J. Select. Areas Commun.*, pp. 1564–1570, Dec. 1995.

[16] R. Price, "Nonlinear feedback equalized PAM versus capacity for noisy filter channels," in *Proc. Int. Conf. Communications*, 1972, pp. 22.12–22.17.

[17] J. G. Proakis, *Digital Communications*, 2nd ed. New York: McGraw-Hill, 1989.

[18] A. Ruiz, J. M. Cioffi, and S. Kasturia, "Discrete multiple tone modulation with coset coding for the spectrally shaped channel," *IEEE Trans. Commun.*, pp. 1012–1029, June 1992.

[19] A. Scaglione, G. B. Giannakis, and S. Barbarossa, "Redundant filterbank precoders and equalizers—Part I: Unification and optimal designs," in *Proc. 35th Annual Allerton Conf. on Comm., Control, and Comp.*, Monticello, IL, Sept. 1997, pp. 385–394.

[20] ———, "Redundant filterbank precoders and equalizers—Part II: Blind channel estimation, synchronization and direct equalization," in *Proc. Int. Conf. ASSP*, Seattle, WA, May 1998, vol. VI, pp. 3501–3504.

[21] M. Tomlinson, "New automatic equaliser employing modulo arithmetic," *Electron. Lett.*, vol. 7, pp. 138–139, Mar. 1971.

[22] X. Xia, "New precoding for intersymbol interference cancellation using nonmaximally decimated multirate filterbanks with ideal FIR equalizers," *IEEE Trans. Signal Processing*, pp. 2431–2441, Oct. 1997.

[23] J. Yang and S. Roy, "On joint transmitter and receiver optimization for multiple-input–multiple-output (MIMO) transmission systems," *IEEE Trans. Commun.*, pp. 3221–3231, Dec. 1994.

[24] T. N. Zogakis, J. T. Aslanis, and J. M. Cioffi, "A coded and shaped discrete multitone system," *IEEE Trans. Commun.*, pp. 2941–2949, Dec. 1995.

[25] W. Y. Zou and Y. Wu, "COFDM: An overview," *IEEE Trans. Broadcast.*, vol. 41, pp. 1–8, Mar. 1995.